Experimental Characterization of Mode I Fracture Toughness of Reinforced Carbon Fiber Laminate with Nano-Cellulose and CNT Additives

Seth D. Berry

Thesis submitted to the Faculty of the

Virginia Polytechnic Institute and State University

in partial fulfillment of the requirements for the degree of

Master of Science

in

Aerospace Engineering

Gary D. Seidel, Chair

Barry S. Goodell

Michael K. Philen

June 27, 2016

Blacksburg, Virginia

Keywords: Delamination, Carbon Fiber, CNT, Nano-Cellulose, Z-pin, Fracture Toughness

Experimental Characterization of Mode I Fracture Toughness of Reinforced Carbon Fiber Laminate with Nano-Cellulose and CNT Additives

Seth D. Berry

(ABSTRACT)

Effective treatment of carbon fiber components to improve delamination resistance is vital to the application of such materials since delamination is one of the biggest concerns regarding the use of composites in the aerospace sector. Due to the significant application benefit gained from increased stiffness to density ratio with composite materials, innovative developments resulting in improved through-thickness strength have been on the rise. The inherent anisotropy of composite materials results in an added difficulty in designing structural elements that make use of such materials. Proposed techniques to improve the through-thickness strength of laminar composites are many and varied; however all share the common goal of improving inter-laminar bond strength.

This research makes use of novel materials in the field of wet flocking and Z-pinning. Cellulose nanofibers (CNFs) have already demonstrated excellent mechanical properties in terms of stiffness and strength, originating at the nano-scale. These materials were introduced into the laminate while in a sol-gel suspension in an effort to improve load transfer between laminate layers. The effect of CNFs as lightweight renewable reinforcement for CFRPs will be investigated. Carbon nanotube (CNT) additives were also considered for their beneficial structural properties.

Experimental Characterization of Mode I Fracture Toughness of Reinforced Carbon Fiber Laminate with Nano-Cellulose and CNT Additives

Seth D. Berry

(GENERAL AUDIENCE ABSTRACT)

In order to ascertain the effects of various nano-material treatment on CFRP delamination resistance, Mode-1 testing was done on DCB coupons made of CFRP pre-preg tape. Mode-1 fracture toughness was used to as the metric of delamination resistance for the various treated specimens. Injection of aqueous suspension of Carbon nanotubes (CNTs) or Cellulose nanofibers (CNFs), using a hypodermic needle, was examined as a possible alternative to traditional z-pinning. Wet-flocking of aqueous CNT and CNF suspensions was also examined as a through-thickness reinforcement technique.

CNF wet-flocking was experimentally demonstrated to increase the mode-1 fracture toughness. CNF injection was not found to provide an increase in the mode-1 fracture toughness. CNT treatments were found to reduce the mode-1 fracture toughness.

Acknowledgments

The author wishes to acknowledge the assistance received throughout this investigation. Without the supervision and guidance of Dr. Gary D. Seidel, and the support of the Aerospace Structural Materials Laboratory's Multi-scale Modeling group, this project would not have been possible. Thank you for letting me stand upon the shoulders of giants. Further, the author would like to thank Jeremy O'Donnell for his invaluable assistance in the lab. Finally, the author would like to thank his parents and friends who provided invaluable support throughout the pursuit of this degree.‘

Contents

List of Figures

List of Tables

Chapter 1

Introduction

1.1 Background

The use of carbon fiber reinforced plastics (CFRP) in primary structural members has happened very slowly. Although CFRPs demonstrate superior mechanical properties in the direction of the fibers, this class of material suffers from weak inter-laminar strength. Efforts to improve the through-thickness strength of CFRP have taken many forms. Z-pinning [3], stitching [4, 5, 6], and other forms of through-thickness fiber reinforcement have been explored as practical methods of increasing composite fracture toughness. Wet flocking is another technique for providing z-axis delamination resistance in composites. This technique consists of introducing nano-scale particles (such as fibers of crystals) between composite layers, dispersed in an aqueous medium, prior to cure. Karwa et al. [7] demonstrated this

technique to produce CFRPs with z-axis reinforcement. Various types of nano-particles have been introduced to composites in an effort to improve delamination resistance [8, 9, 10].

The development of an effective Z-pin medium with focus on improved Mode I fracture toughness in carbon fiber could provide a robust solution to current industry limitations for availability and renewability of composite materials. This research will make use of Cellulose nanofibers, a novel material in the field of composite laminates and Z-pinning. Since these materials are injected into the laminate while in a fluid form, their presence between the fabrics of each layer will effect load transfer. These z-pin-like structures will be examined to see if they can provide the nominal strength required to resist delamination in composite laminates.

1.2 Research Objectives and Approach

The objective of this research is to examine the effects of the addition of Cellulose Nano-fiber (CNFs) and Carbon Nano-tubes (CNTs) on the mode 1 delamination resistance of CFRP sample coupons. In this work, various methods of introducing the CNFs and CNTs will be compared using Double Cantilevered Beam (DCB) tests in accordance with ASTM D6628 [11]. Woven carbon fiber pre-preg (0-90 weave) will be laid up in a rectangular sample consisting of 20 layers. A pre-crack will be formed by placing an insert between the two middle layers (10-11) along one side of the sample. The sample will be placed in a press and cured at 177 degrees Centigrade for six hours. The cured plate will be cut into DCB test

coupons. Aluminum mount blocks will be adhered to the top and bottom of the sample on the pre-crack side using epoxy. The fracture toughness of the various treated specimens will be compared with that of neat samples.

CNFs and CNTs will be introduced either using a wet flocking technique or by injection using a hypodermic needle. For both methods, the Mode 1 fracture toughness will be compared with that of neat samples to determine whether an improvement in mechanical properties occurred as a result of the treatment. Specimens treated with CNTs will be tested for improvement in mechanical properties. The mode 1 fracture toughness of treated specimens will be compared with that of neat specimens.

The injection of nano-material into composite pre-preg is designed to emulate traditional z-pinning techniques. Instead of introducing fibers in the Z-axis, the nano-material is intended to form areas of increased through-thickness strength in the area around the injection. These cylindrical regions of nano-materials are designed to mimic traditional z-pins.

The wet-flocking technique for introducing nano-materials into composite pre-preg is designed to concentrate the material at the interlaminar bonds, where the composite is weakest, in order to improve delamination resistance of the pre-preg material during the layup process.

A set of DCB coupons with carbon fiber stitched through the z-direction will be used as a point of comparison. These samples will exhibit the behavior expected of traditional z-pinned DCB specimens.

Chapter 2

Literature Review

This review is divided into four sections, each dealing with a separate aspect of this research. The first three deal with aspects of the test procedure, and the last describes nano-cellulose preparation.

2.1 DCB test

The Double Cantilevered Beam test (DCB) is described in ASTM standard D6682 [11]. P Robinson et al. described mode-1 delamination testing of multi-directional CFRP laminates [12]. The test was originally designed for testing composites with linear fibers aligned along the length of the specimen. Because a multi-directional 0-90 weave composite is less likely to have fiber bridging between the delaminated layers, the behavior of such materials in Mode 1 testing can vary from what would be expected for linear fiber composites. Bradley

et al. [13] found that fiber breakage, fiber bridging and ply jumping were most significant in specimens with angles other than 0 and 90 degrees. In these cases, they found that the fracture toughness ceased be an accurate measure of delamination resistance. When 0-90 weave fibers were used, these effects were less pronounced. In this work, 0-90 weave CFRP was used, and no fiber bridging or ply jumping was observed during testing.

The effect of varying loading rates for DCB testing was examined by S. Mall [14] with the Air Force Institute of Technology, as well as by Jacob et al [15] and Smiley and Pipes [16]. These studies consistently found that dynamic effects can reduce the accuracy of the tests at higher crosshead rates. The ASTM standard allows rates between 1 and 5 mm/min. In order to avoid dynamic effects during the test, a rate of 1mm/min was used in this work.

2.2 Crack tracking

In order to calculate fracture toughness during the DCB test, the crack propagation must be known throughout the test. Several methods for achieving this have been proposed. Yarlagadda et al. [17] proposed using Time-Domain Reflectometry (TDR) in which an in-situ embedded sensor running the length of the specimen was used to observe crack propagation measurements. They compared the results with the more traditional visual measurement, and found a very good correlation. Fig. 2.1 shows the correlation between the TDR measurements and the visual measurements of the crack length during three DCB tests.

With the excellent correlation between TDR and visual observation, neither technique was

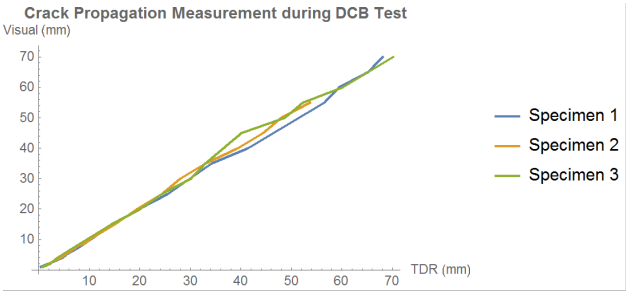

Figure 2.1: TDR measurements and the visual measurements of the crack length during three DCB tests. Values for plotting are taken from An Automated Technique for Measuring Crack Propagation during Mode I DCB Testing, Yarlagadda, et al.

found to be substantially more accurate, although additional care is needed when visually tracking the crack growth in order to avoid isolated variation [17]. TDR provided automated crack length data, but required additional effort during specimen layup, as well as the additional cost of the sensor. Considering the limited benefits and increased cost and effort of TDR, this work used the visual crack tracking method, and a computer code (Appendix **??**) was written to provide a user interface for extracting crack length from video of the test. This technique is described in section 3.5.

2.3 Fracture Reduction

Ranatunga and Clay [18] described z-pinning from both the experimental and modeling perspective. Cartie and Partridge [19] described advanced z-pin manufacturing techniques, and demonstrated them experimentally.

Traditional Z-pinning and similar Z-direction reinforcement techniques generally provide improved out-of-plane strength at the cost of in-plane strength. As the density of the pins or stitches increases, the Z-direction toughness generally increases, while the in-plane properties are increasingly degraded [20, 21]. Blanco et al. [22] proposed that using nano-scale additives at the laminar interfaces by a wet flocking technique which may provide an increase in through-thickness strength without compromising in-plane material properties.

2.4 CNF processing

Cellulose is a renewable bio-polymer which is found abundantly in nature. It is a semi-crystalline polysaccharide which has both crystalline and amorphous regions. Cellulose fibers have lengths ranging from 0.5μm up to several millimeters, and widths ranging from 5 to 20 μm. fig. 2.2 shows the structure of cellulose in wood. The octagonal shapes represent the individual glucose molecules which make up the cellulose polymer. Chains of 50 glucose molecules make up an individual cellulose molecule. These bundle together into either a crystalline or amorphous structure, and are bonded to each other and to lignin molecules by hydrogen bonding and other inter-molecular forces.

Cellulose nano-materials have been proposed as a beneficial additive to CFRPs because of their availability, high strength to weight ratio, sustainability, and biodegradability. Nano-scale cellulose can be found in both fiber and crystal forms, and can be derived from plant-based sources as well as from bacteria. Publications concerning nano-cellulose applications in

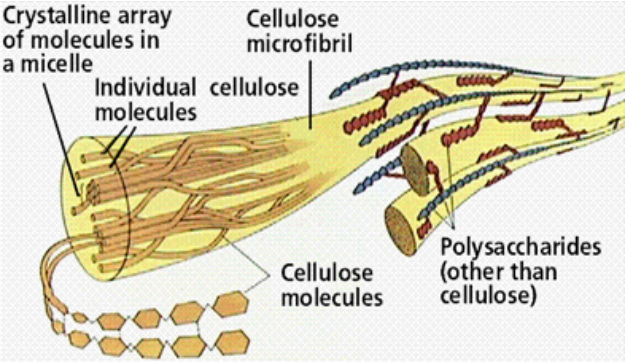

Figure 2.2: Schematic of Cellulose fiber bundling (Sinauer Associates, Inc. Used by permission) [1].

composites saw a sharp rise in the early 2000s, with a corresponding increase in patents [2]. Table 2.1 describes various nano-scale cellulose particles. The properties of these materials depends on the scale and aspect ratio of the particles.

Micro-fibrillated cellulose is a type of cellulose nano-fiber (CNF) that is prepared by mechanically shearing cellulose bundles to expose nano-scale fibers. Herrick et al. [23] and Turbak et al. [24] used high pressure cyclic mechanical shearing to disintegrate wood pulp into cellulose micro-fibrils, resulting in CNF gel with a high degree of entanglement between fibers. The fibrillation process is often accompanied by chemical pre-treatments which aid in breaking down the cellulose bundles exposing individual nano-cellulose strands. These pre-treatments were found to reduce the energy required to manufacture CNFs via nano-fibrillation [25].

Alamri and Low [26] described the thermal and mechanical properties of cellulose fibers in epoxy resin. Karima Ben Hamou et al. [27] studied polyurethane reinforced with nano-scale cellulose crystals and fibers. Akira and Saito [28] described the process of TEMPO-mediated

Table 2.1: Nano-cellulose dimensions (Samir et al. 2005; Tanem et al. 2006; Hubbe et al. 2008) [2]

Cellulose structure	**Length (nm)**	**Aspect Ratio (L/d)**
Microfibril	>10,000	>1,000
Microfibrilliated Cellulose (MFC)	>1,000	100-150
Cellulose Whisker	100-600	10-100
Microcrystalline Cellulose (MCC)	>1,000	1

oxidation used to break chains of cellulose into nano-scale fibrils with extremely high aspect ratios. This method was used to prepare the CNFs used in this work.

Chapter 3

Experimental Methods

DCB specimens were manufactured in accordance with ASTM D6628 [11]. A summary of this process is shown in fig. 3.1. The CFRP specimens were made from pre-preg using the Cycom 977-2 Resin System (a). The pre-preg was laid up by hand (c) and cured in a MTI EQ-DZF-6020 vacuum oven (f). The cured CFRP was cut into individual sample coupons and aluminum mounting blocks were affixed using DP-460 epoxy (h). The finished specimens underwent Mode-1 delamination on an MTest Quattro testing frame (i). A Samsung video camera was used to record the tests.

3.1 Nano-material Preparation

Some samples were treated with nano-materials prior to cure, either via direct injection after layup, or by wet flocking during layup. Both CNF gel and CNT suspensions were used.

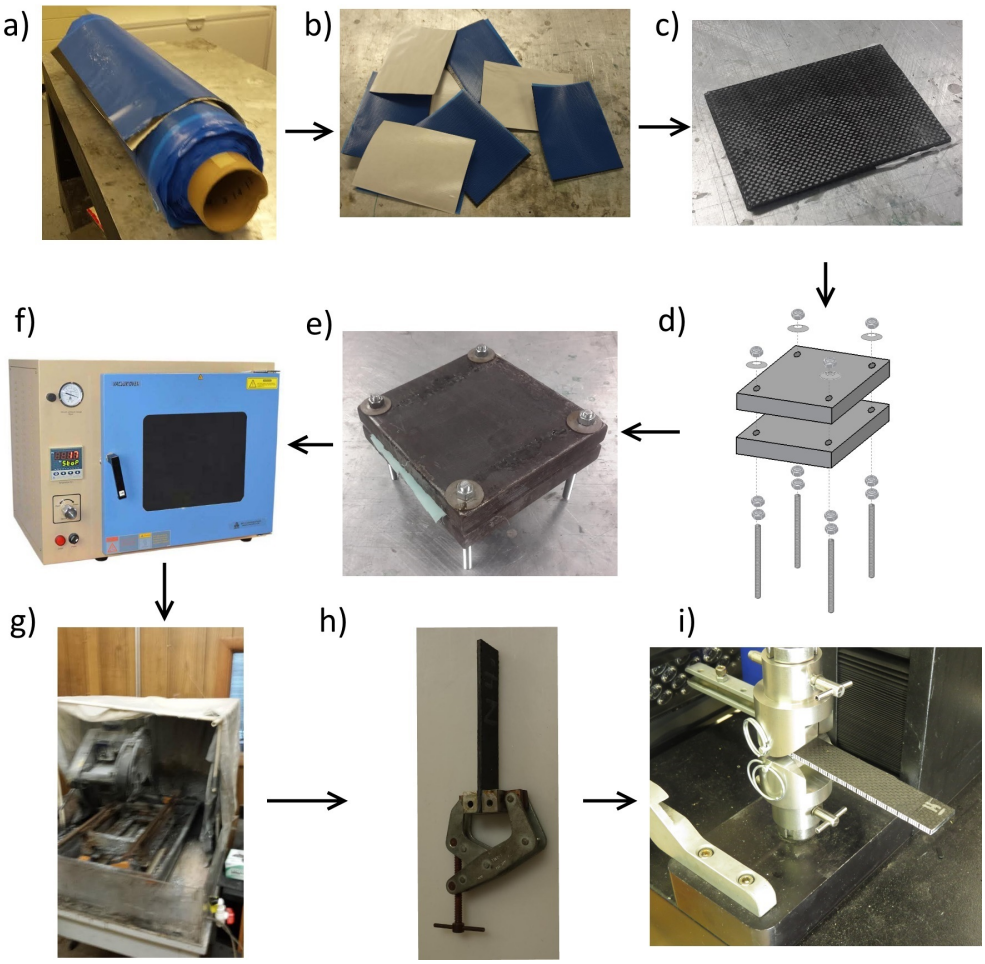

Figure 3.1: Summary of the experimental method showing sample preparation, curing, assembly, and testing. a) Pre-preg roll, b) pre-preg layers, c) pre-cure layup, d) press assembly, e) press with sample, f) cure oven, g) diamond wet saw, h) specimen with mounting blocks in clamp, i) specimen mounted on testing frame

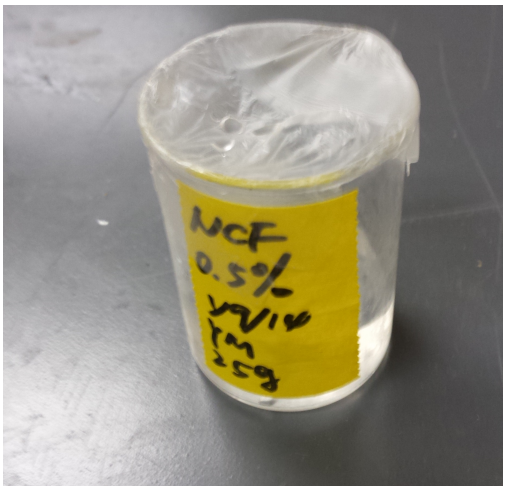

Figure 3.2: CNF gel suspension.

3.1.1 CNF Preparation

The CNFs were prepared using a TEMPO-mediated oxidation process, in which an oxidation agent was introduced to reduce the amount of energy necessary to break apart the cellulose bundles and expose individual fibers. The CNFs were suspended in distilled water to form a gel. The concentration of the CNFs was between 0.8% and 1.0% by weight. Fig. 3.2 shows the CNF gel suspension used in this work. The gel was prepared by TEMPO-mediated oxidation.

The CNFs in this work were prepared by the Virginia Tech Sustainable Biomaterials Department at the Institute for Critical Technology and Applied Science[1].

[1]Goodell Lab Sustainable Biomaterials and Bioenergy. ICTAS II. Life Sciences Circle, Virginia Tech

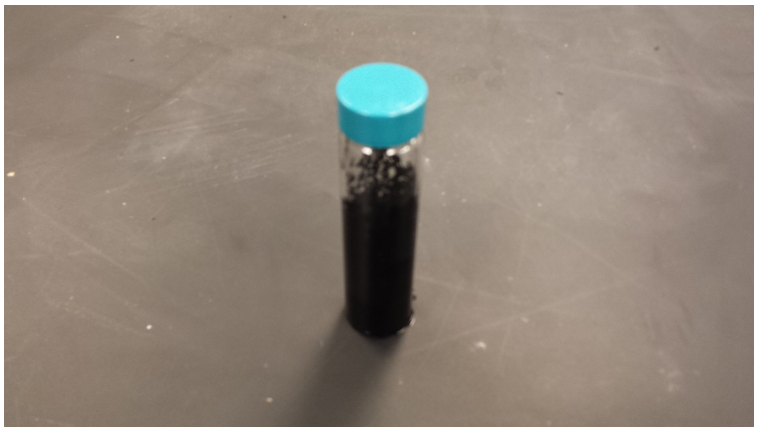

Figure 3.3: CNT suspension in distilled water.

3.1.2 CNT suspension

Single Walled CNTs were suspended in distilled water using an ultra-sonification device. The CNTs were 40-60 percent carbon, by weight. The weight concentration of the CNT suspension was 0.05%. The CNTs were added to distilled water in a test tube and dispersed via ultra-sonification for one hour. Fig. 3.3 shows the CNTs suspended in distilled water after ultrasonification.

3.2 Pre-preg Layup

3.2.1 Neat Sample Technique

20 layers of CFRP tape were laid up in a rectangle measuring 4"x5.5". A PTFE insert was placed at one end of the layup between layers 10 and 11. The insert extended two inches

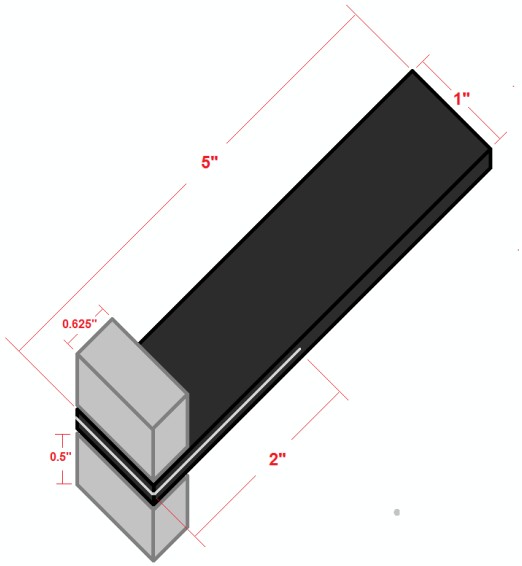

Figure 3.4: Schematic of a DCB Test Coupon showing dimensions.

from the edge. The rectangular layup was pressed between two steel plates with a layer of release film separating the plates from the carbon fiber. These plates were equipped with four threaded rods running through holes at each corner. A nut and washer assembly was used to compress the two steel plates. A force transducer was used to find a correlation between torque applied to the assembly and the corresponding pressure applied between the two plates, allowing the plate pressure to be controlled by controlling the torque. The four nuts were equally tightened to 33 ft-lbs using a mechanical torque wrench. This corresponded to a pressure of 57 psi on the composite layup.

This assembly was then cured in an oven at 177 degrees Celsius for 6 hours. Two hours into the cure, the assembly was retightened to 33 ft-lbs. This was necessary due to thermal expansion which caused a reduction in the pressure applied by the plates. Once the cure was completed, the assembly was removed and allowed to cool. Once separated from the plates,

the cured rectangular composite was cut into rectangular sample coupons measuring 1"x5" with the 2" PTFE insert at one end of the sample. Fig. 3.4 shows the dimensions of the test coupon. Specimens were initially cut using a band saw, but an improvement in quality of cut was observed when a diamond wet saw was used. At the end with the PTFE insert, 80-grit sandpaper was used on the top and bottom to prepare the surface for bonding. An aluminum block measuring 1"x0.5"x0.625" was mounted onto the specimens using DP-460 epoxy. The samples were placed in a clamp and allowed to set overnight. Light sanding of the area around the block was then done using 220-grit sandpaper in order to remove any stray epoxy.

3.2.2 Stitched Carbon Fiber Technique

Two samples were made and tested with carbon fiber z-pins. After sample layup, but prior to cure, an awl was used to puncture holes through the sample, and a sewing needle (diameter 0.7 mm) was used to sew thread carbon fiber yarn through the sample in the Z-direction. The thread was then cut off, and this process repeated, with a pin approximately ever 1/4" along the sample's width. Three rows of pins were added, each 0.75" apart, starting 0.75" from the end of the pre-crack as shown in fig. 3.5.

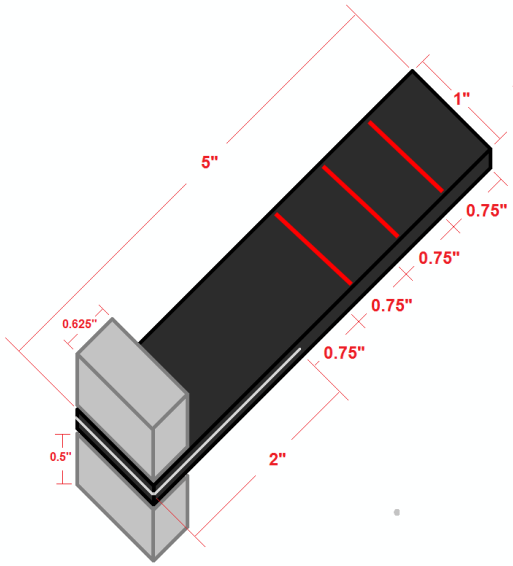

Figure 3.5: Schematic of a DCB Test Coupon showing location of zpins.

3.2.3 Injection Treatment

In order to prepare samples with various treatments, the procedure described in 3.2.2 was modified slightly. In order to prepare samples injected with CNFs, a template was placed over the portion to be treated after layup, but prior to cure. This template consisted of a thin flat plate with holes in a grid pattern. Figure 3.6 shows the template. An awl was used to puncture small holes vertically through the material. Once the hole was made, a hypodermic needle (diameter 0.4 mm) was used to inject nano-material. Three rows were added, each 0.75" from the previous, with the first row beginning 0.75" from the end of the PTFE insert as shown in fig. 3.7.

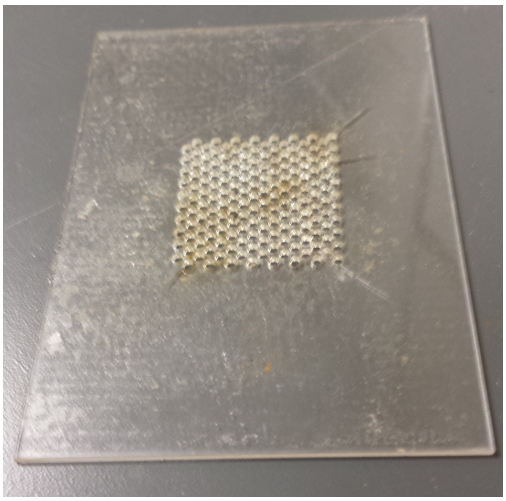

Figure 3.6: Injection template plate used to align injected z-pins.

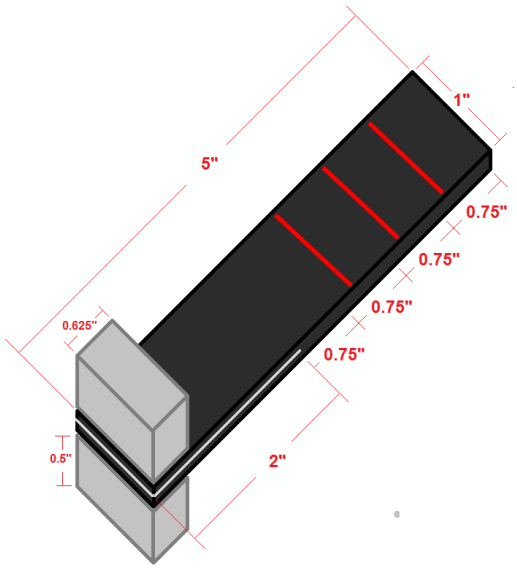

Figure 3.7: Schematic of a DCB Test coupon showing location of injected CNFs.

3.2.4 Wet-flocking treatment

Another technique for introducing the CNF or CNT additives to the composite was to add a thin layer of the nano-material between each layer of pre-preg tape. In this method, referred to as wet-flocking, the treatment was applied during layup. After each 4"x5.5" rectangular layer of pre-preg tape was put into place, nano-material was spread evenly over the area to be treated. The material was added between each of 20 layers. In the case of CNF gel, this was accomplished by spreading the material using a hard plastic card. In the case of CNT suspension, the suspension was sprayed directly onto the surface using a misting spray bottle. The nano-cellulose was added beginning 0.75" from the end of the PTFE tape, and extending to the end of the sample as shown in figure 3.8. The CNT suspension was applied over the entire surface of the specimens. Samples were treated with either nano-cellulose or CNTs.

3.2.5 Injection-Control Treatment

In order to determine whether any change in mechanical properties could be attributed to fiber displacement during the injection process, a set of samples was injected with the awl, but no additive was injected. These samples are referred to as the injection-control group in this work.

By puncturing the pre-preg fabric with the needle, but not injecting CNF gel or dispersed CNTs, it was possible to separate the effect of fiber displacement from that of the added

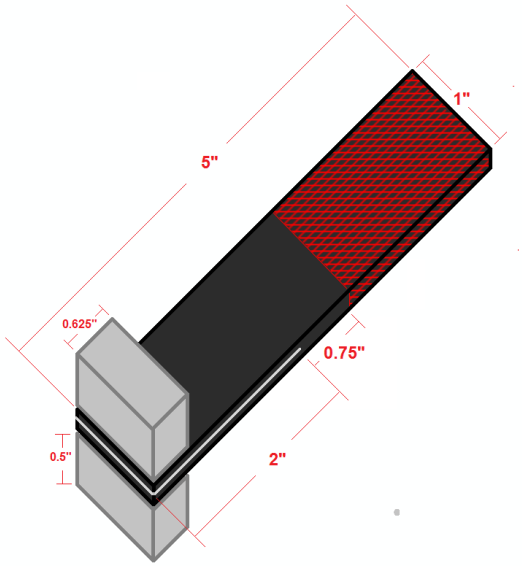

Figure 3.8: Schematic of a DCB Test Coupon showing location of wet flocked CNFs.

nano-material. These samples were prepared in exactly the same manner as the injected CNF samples, except that no material was added. The same template plate shown in figure 3.6 was used.

3.2.6 Water-Control Treatment

Because both the CNFs and CNTs were suspended in water, a sample set was made to determine the effect of the water on the material's properties. The Water-control group consisted of samples treated with water during layup. The procedure was exactly the same as the CNT wet-flocking technique, except that the misting bottle was filled with pure distilled water instead of an aqueous CNT suspension. This sample set, then, could be thought of as being treated with "zero weight" CNT wet-flocking. The purpose of the water-control group

was to separate the effect of water in the supsension from that of the nano-materials being added.

A similar control group consisting of samples made by injecting pure water using the syringe was proposed, but this control was not used in this work since it would have been difficult to separate the effect of the injected water from that of the fiber dislocation itself. For this reason, only the injection control and water control are presented in this work.

3.3 Sample Curing

Once the layup was complete, the sample was clamped within a press. A nylon release film was used to separate the sample from the steel plates on the top and bottom. This press consisted of two steel plates with holes at each corner. Two nuts were threaded onto the end of a length of threaded rod. The rod was inserted through both steel plates, and then a Belleville washer was added and a third nut threaded onto the upper end of the rod. This thread assembly was repeated for each of the four corner holes. The press assembly was tightened to 33 ft-lbs using a torque wrench.

The press was then placed in a curing oven for six hours at 177 degrees Celsius in accordance with the recommended cure schedule. Two hours into the cure, the press was removed and re-tightened to 33 ft-lbs.

Re-tightening was necessary as the pressure applied by the press was found to be inconsistent during initial cures. A test was performed to determine the cause of this loosening, and it was

found that it was most likely due to thermal expansion rather than to slipping of the threaded assembly. During this test, the press was re-tightened every hour throughout the cure. It was determined that after two hours there was no significant lessening of the pressure, and the press maintained a constant pressure for the remainder of the cure.

3.4 Test Coupon Preparation

Once the six hour cure was complete, the press was removed from the oven and allowed to cool overnight. The thread assembly was then removed, and the press was pried open. Once removed, the CFRP plate was marked with a grease pencil along cutting lines. Three sample coupons were cut from each plate. The coupons measured 5"x1" aligned such that the PTFE insert would extend two inches from the samples edge in accordance with ASTM standard D5528. A band saw was found to make cuts of acceptable quality, but the best quality cuts were obtained using a diamond wet saw.

The test coupons were then lightly sanded and cleaned to remove dust. Along the side with the PTFE insert, the top and bottom was sanded for about 0.5" with 80 grit paper to prepare the surface for adhesive. The surface of the aluminum mount blocks was similarly sanded, cleaned and prepped for bonding. DP-460 epoxy was used to bond the mount blocks to the test coupons. The finished samples were then kept in a clamp overnight. Finally, the edges of the sample around the PTFE insert were lightly sanded with 220 grit sandpaper to ensure no stray epoxy had dripped onto the pre-crack. This was found to drastically improve the

quality of the pre-crack and prevent high initiation toughness.

3.5 Mode 1 Testing

The samples were pinned to an Mtest Quattro testing frame as shown in fig. 3.9. A video camera was positioned to capture the fracture test edge-on. The crosshead control was moved at a constant rate of 1mm per minute throughout the test. This rate is within the range advised by the ASTM standard [11], but is toward the lower end of the acceptable range. This slower rate was determined to be preferred so as to minimize dynamic effects in the test. Several studies found that higher rates of crosshead displacement can result in an apparently lower fracture toughness due to dynamic effects [14, 15, 16]. Similarly, early tests performed at higher rates led to lower quality data.

Crosshead displacement and specimen loading were measured using the Mtest Quattro testing frame. Crack propagation data was obtained from the video of the test. A Panasonic HC-V750 video camera was positioned in a tripod approximately two feet from the sample being tested. A light source was positioned to the left of the camera, directed into the open crack. A silver permanent marker (sharpie^{TM} brand) was used to color the sample edge to improve crack detection.

A code written in Mathematica was used to extract frames from the video file for processing. This code provided a user interface for selecting the location of the crack tip. With appropriate calibration, this input was used to determine the crack length. Using the first frame

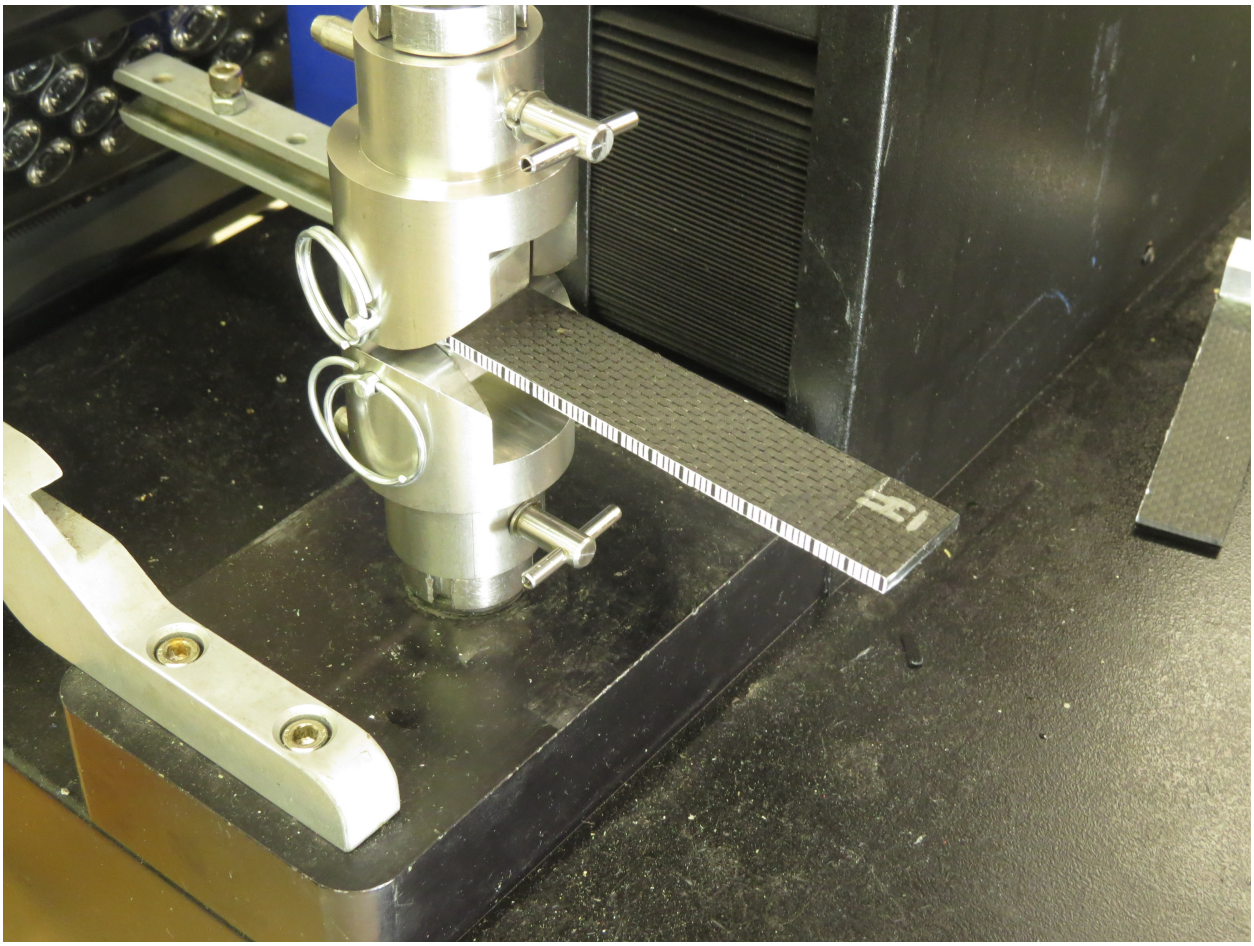

Figure 3.9: DCB sample coupon mounted in the Mtest Quattro testing frame.

from the video, which was prior to the start of the test, the user clicked with the mouse on the left and right ends of the sample. Using this calibration, the code associated the mouse position with the corresponding location along the sample. With every click of the mouse a data point was taken, and the next frame was displayed. A datapoint was taken every four seconds from the video file. Fig. 3.10 shows several frames from a test video and their corresponding locations on the crack-length plot. The code is presented in Appendix **??**.

The test was continued until sample breakage occurred. Crack data was then extracted from the video file as described above, and the resulting crosshead displacement, load and crack length data were used to determine plots of fracture toughness.

3.6 Cure Pressure

An ideal cure pressure was not provided with the pre-preg used, and could not be obtained from the manufacturer. In order to determine whether cure pressure would significantly affect the properties of the samples, a set of neat samples was made at three different pressures. The 14.7 and 54 psi samples were made in the press described in Section 3.3, but since the press could not accommodate a pressure of 90 psi, a hydraulic hot press was used to cure the 90 psi sample set. This hot press could not be used for the remaining testing as it was found not be able to hold a constant pressure, and its minimum measured pressure was 2,000 pounds. Fig. 3.11 shows the crosshead load plotted against the crosshead displacement for each of three characteristic samples cured at the three cure pressures.

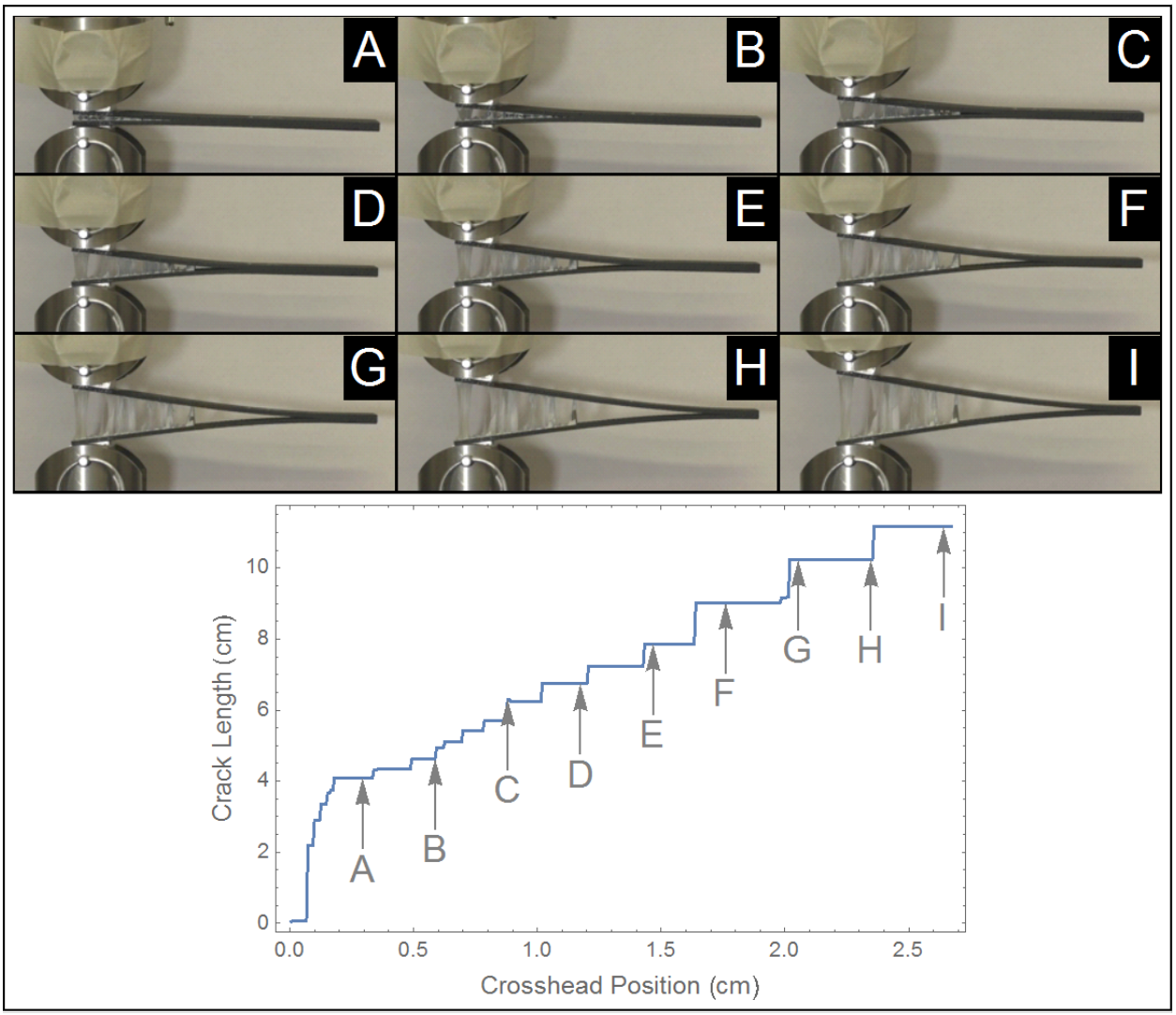

Figure 3.10: Sample video frames showing crack progagation and corresponding plot of crack length vs. cross-head displacement.

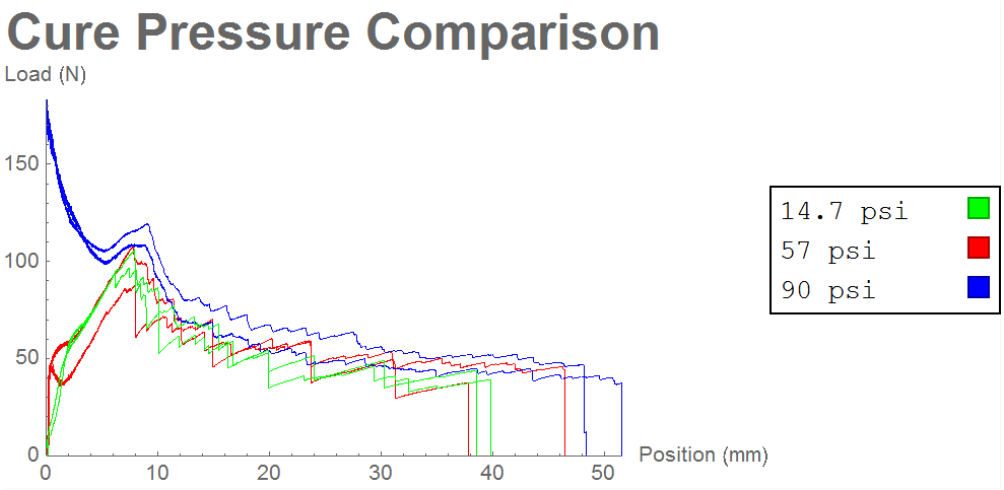

Figure 3.11: Plot of Load vs. Crosshead displacement for samples cured at 14.7, 57, and 90 psi.

Although a slight increase in load was observed, it was not enough to warrant using the less precise press. The inability of the hot press to maintain a constant pressure made it unsuitable for obtaining reliable results. The cure pressure of 57 psi was used for all specimens in this work, as that was found to be sufficient.

Chapter 4

Observations

A MATLAB script was written to plot the crosshead load and crack length against the crosshead displacement. The script then generated a fracture toughness plot using the data. Characteristic figures are shown for each specimen type below. A figure showing uncertainty for each sample type is presented, and a plot of the fracture toughness for multiple specimens of each type is shown. Finally, a comparison is shown between each specimens type is shown.

Figure 4.1 shows a schematic of the DCB specimen with the nomenclature used in the ASTM standard. The thickness, width and length of the specimen are shown, along with the crack length, crosshead displacement, and crosshead load. This nomenclature is used in the calculation of fracture toughness.

Table 4.1 summarizes the specimens made and tested.

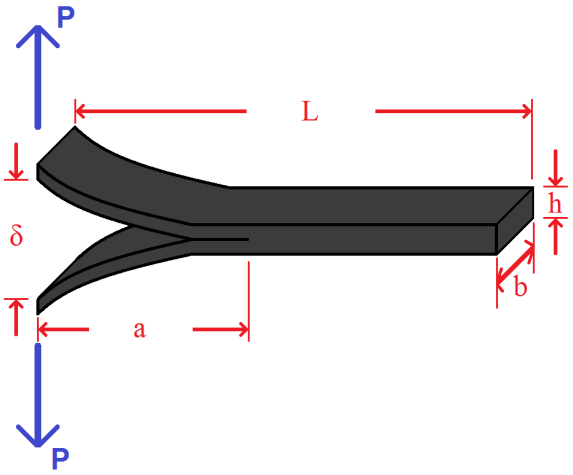

Figure 4.1: Schematic of a DCB Test Coupon showing the nomenclature used in the ASTM standard .

Table 4.1: Summary of Specimen Types.

Sample	Number Tested	Description
Neat	5	Untreated Mode 1 DCB sample
3-row CNF	8	Injected with CNF get in three rows
3-row CNT	2	Injected with CNT suspension in three rows
Wet flocked CNF	6	Wet flocked CNF gel between each layer
Wet flocked CNT	3	Wet flocked CNT suspension between each layer
Injection-Control	3	Holes punctured with awl without injecting material
Water-Control	6	Water sprayed between each layer

4.1 Crack Length Uncertainty

In order to estimate the precision with which the crack length could be extracted from a video of the test, the crack tracking code was run multiple times for one test video. This code, described in 3.5, was a user interface designed to allow the user to click on the crack tip within consecutive video frames. The code then outputted the crack length, as a function of time. By running the code multiple times, it was possible to estimate how consistently the user could identify and click the crack tip.

Figure 4.2 shows the results of this analysis. The code was run, using the same test video, multiple times by multiple users. The results seems to be very consistent between runs, suggesting that the crack tracking code provides a means to precisely measure crack growth in a DCB specimen.

4.2 Tensile Tests

In order to determine the in-plane material properties of the CFRP used in this work, two rectangular specimen measuring 5"x1" was made with 20 layers of pre-preg. Strain gauges were applied to the specimens in the axial and transverse directions. The specimens were subjected to a tensile load, and the stress-strain response was observed. Figure 4.3 shows this response with the standard deviation based on five tests. Figure 4.4 shows the axial vs. the transverse strain on the specimen, with the standard deviation based on five tests. The

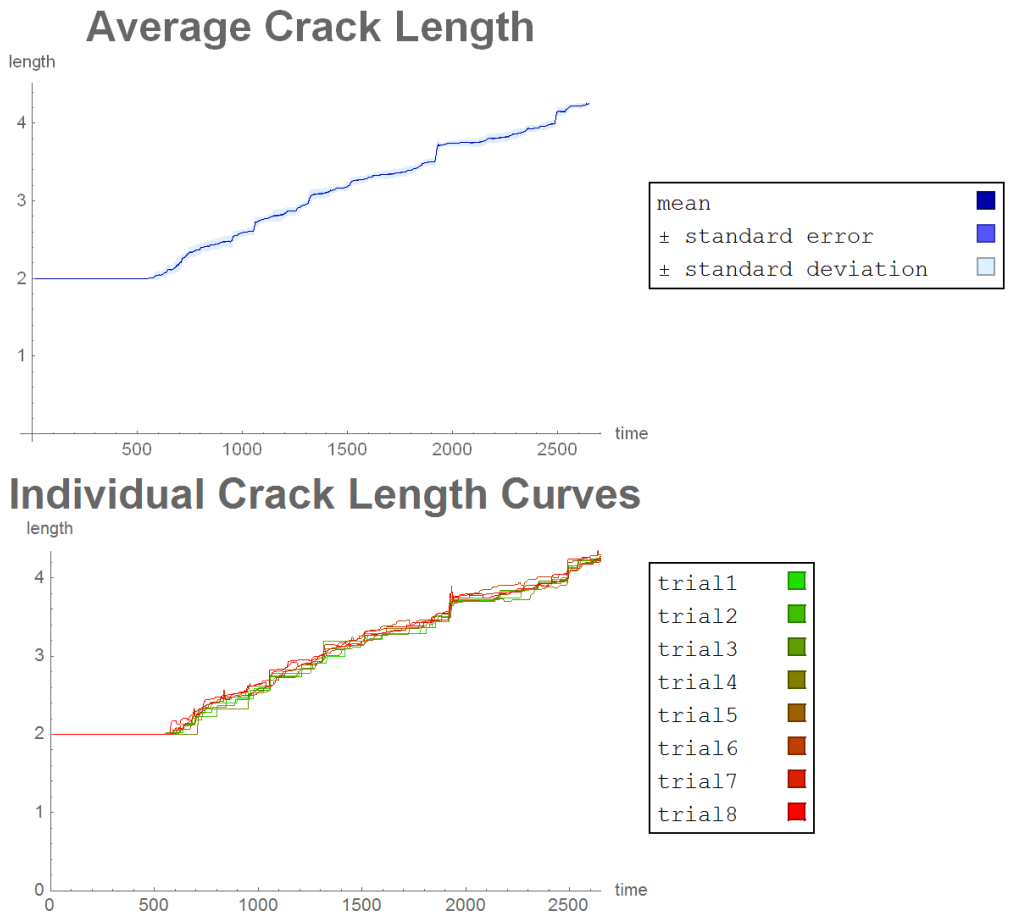

Figure 4.2: Average crack length vs. time, with Standard Error and Standard Deviation (top) and crack length vs. time for a single neat DCB specimen, run multiple times through the crack tracking code.

slope of the curve in figure 4.3 is the Young's Modulus, and is 60.6173 Gpa. The slope of the curve in figure 4.4 is the Poisson's Ratio, and is 0.0724.

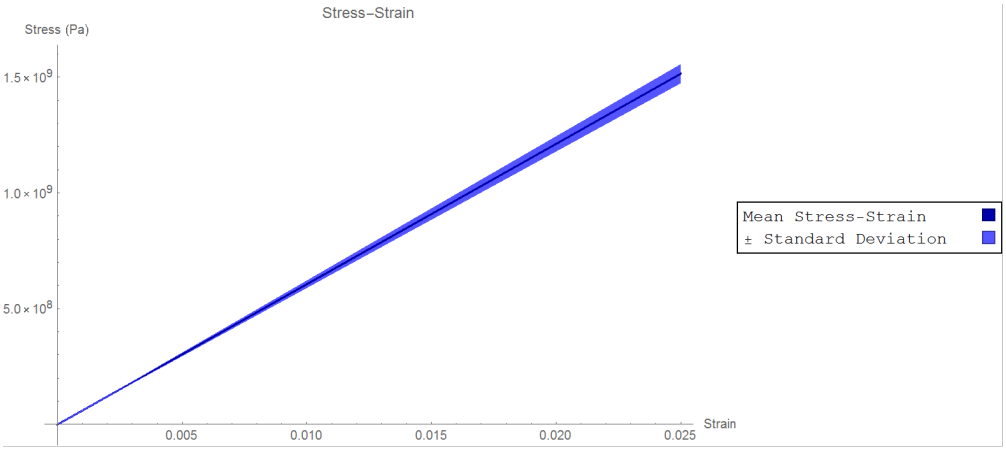

Figure 4.3: Plot of Stress vs. Strain for Cycom 977-2 Resin CFRP pre-preg.

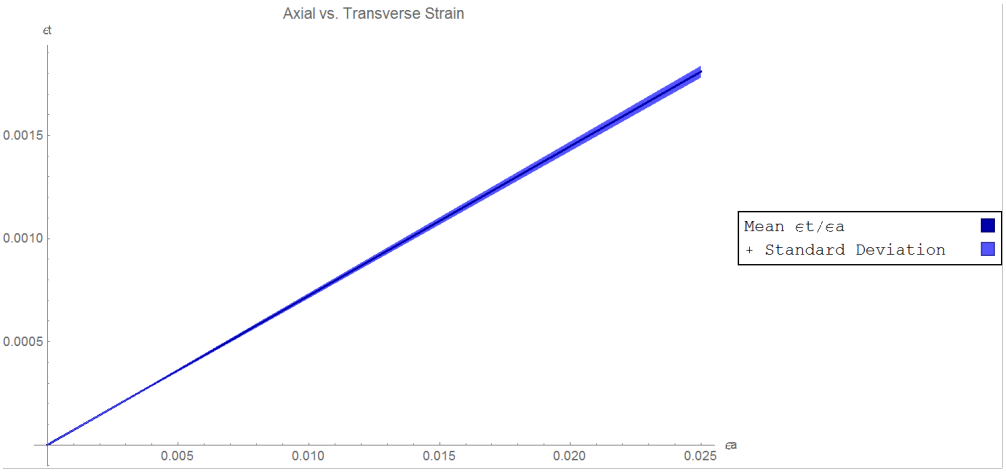

Figure 4.4: Plot of Axial vs. Transverse Strain for Cycom 977-2 Resin CFRP pre-preg.

The carbon fiber fabric was 0-90 weave with even weave in the warp and weft. This means that the material has a plane of symmetry and E_{xx} and E_{yy} are the same. The z-direction modulus, E_{zz}, was not determined.

4.3 Neat Samples

Neat, or untreated samples were made as described in section 3.2.1. These specimens form the primary control group, and provided a baseline with which to compare changes in mechanical properties associated with the various treatments. The specimens measured 1"x5". They had a two inch pre-crack made using a Teflon insert at one end. Two aluminum blocks were affixed to the samples so they could be mounted to the testing frame.

4.3.1 Characteristic Results

The crosshead load and crack length were plotted against crosshead displacement on the same figure. The crack length scale appeared on the left, and the crosshead load scale appeared on the right of the figure. The load plots consistently demonstrated a sharp rise to a maximum peak followed by a series of releases and loadings as the crack traveled along the length of the specimen. The initial load peak is caused by a higher initiation toughness. This initiation toughness varies widely from sample to sample, and depends greatly upon the quality of the pre-crack.

Throughout the test, the crack growth was consistently found not to progress at a constant rate. Rather, the crack length would remain constant for a period of time building up strain energy, and then would suddenly release, traveling a small distance along the length of the specimen. A corresponding pattern was found in the crosshead loading, which exhibited periods of quasi-linear loading (corresponding to regions of constant crack length) followed

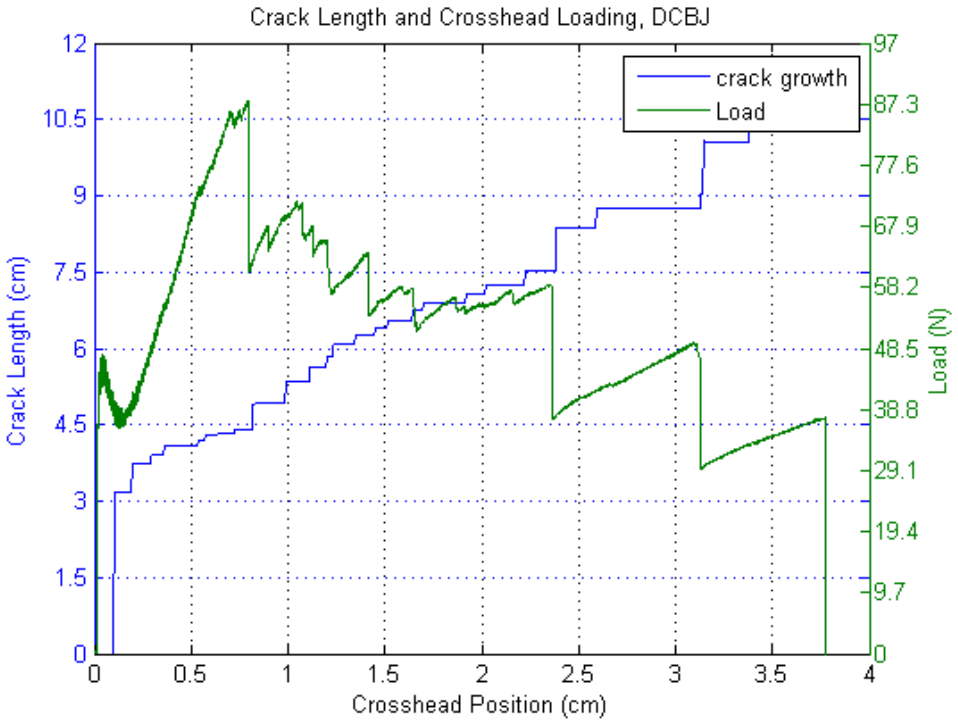

Figure 4.5: Crack length and crosshead load vs. crosshead displacement, neat sample.

by sudden drops in load (corresponding to sudden crack growth). The crosshead load and displacement were recorded by the ADMET testing frame. The crack length was extracted from a video recording of the test. Fig. 4.5 shows the load and crack length plotted against the crosshead displacement for a neat sample.

The crosshead load reaches a peak value at a crosshead position of about 0.8 cm. After this peak, the plot is characterized by repeated loading and release phases. At a crosshead position of about 3.75 cm, the crack suddenly advanced to the end, causing the test coupon to break. This was characteristic of every test performed. After the crack had grown to a certain length, the sample would suddenly and violently delaminate the rest of the way.

4.3.2 Uncertainty

A higher margin of uncertainty is inherent in the nature of fracture testing than in tests which remain in the linear region of a materials stress-strain curve. A statistical measure of the error inherent in the DCB testing is therefore necessary. In order to determine the uncertainty in the results, a plot of averaged values from multiple tests was constructed. Once a sample failed, its contribution to the average was removed. In other words, if a particular sample failed before any others, the average of future data points was calculated only using the remaining samples, rather than including a zero value (for the finished test) in the calculation. This code is presented in **??**

Figure 4.6 shows a plot of crosshead load vs. crosshead position for several neat sample tests. The top graph shows a plot of the averaged values at each crosshead position and a band showing Standard Error and a band showing one standard deviation from the average. The bottom graph shows data for five neat samples.

There is a slightly higher error during the initiation phase which is due to the inherent variability of the pre-crack. After the initial peak value, however, the error is reduced, and remains relatively constant for the remainder of the test.

4.3.3 Fracture Toughness

Using the nomenclature in fig. 4.1, the fracture toughness is calculated using the following equation. The fracture toughness is a standard measure of delamination resistance, and is

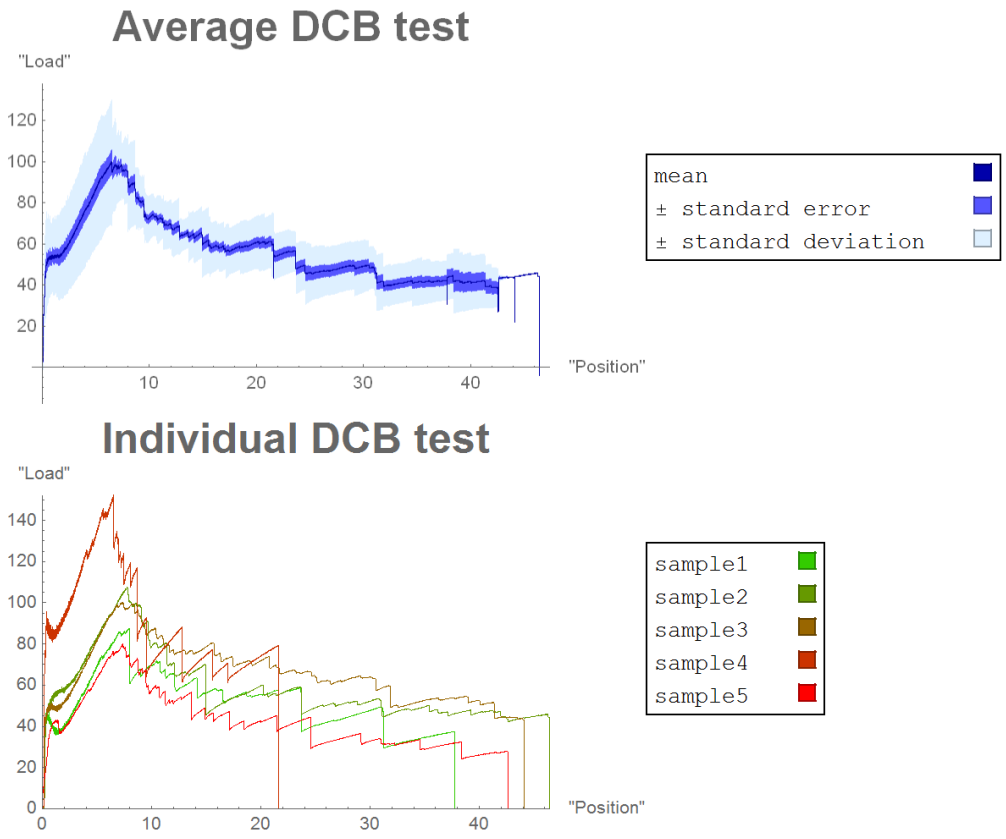

Figure 4.6: Average crosshead load vs. crosshead position, with Standard Error and Standard Deviation (top) and crosshead load vs. crosshead position for several individual DCB tests (bottom), for neat DCB specimens.

described in the ASTM standard. P is the crosshead load, δ is the crosshead displacement, a is the crack length, and b is the specimen width.

$$G_I = \frac{3P\delta}{2ba}$$

A MATLAB script was created to plot the fracture toughness against the crack length. Because the crack demonstrated a pattern of loading phases followed by sudden releases, the

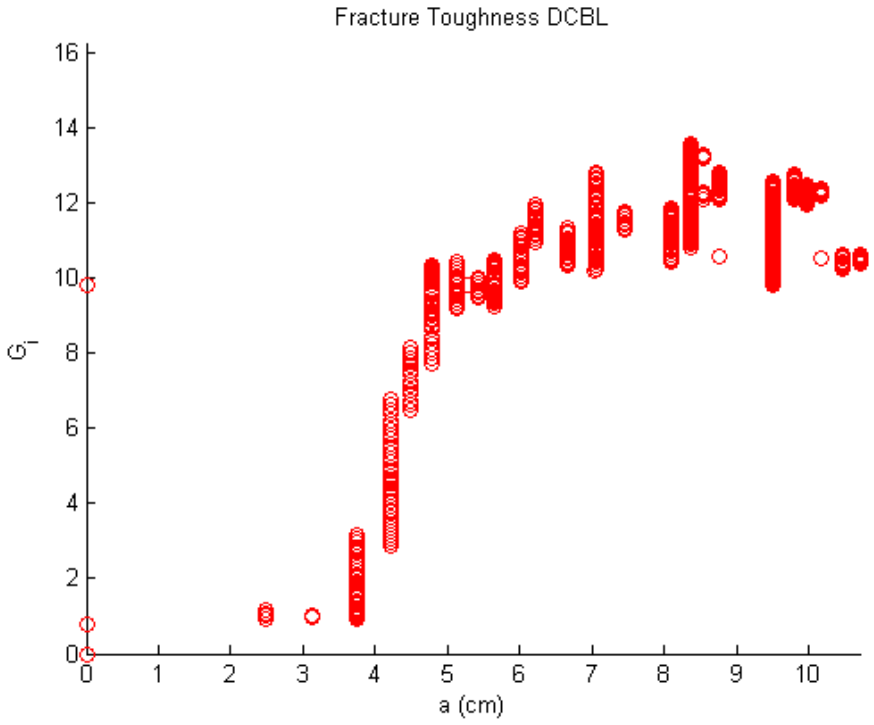

Figure 4.7: Fracture Toughness at each data point, showing the rise in fracture toughness during loading phases.

data points in the fracture toughness plots appeared as a series of vertical lines. This was because the crack length remained constant during these loading phases, while the strain energy increased. Only the top-most point in each column of points was of interest, since this represented the highest fracture toughness at a given point and corresponded to the fracture toughness right before a release phase. Fig. 4.7 shows an example of the fracture toughness at each data point.

The unnecessary points were removed from the plots, showing only the highest fracture toughness achieved for a given crack length. Fig. 4.8 shows the fracture toughness for the

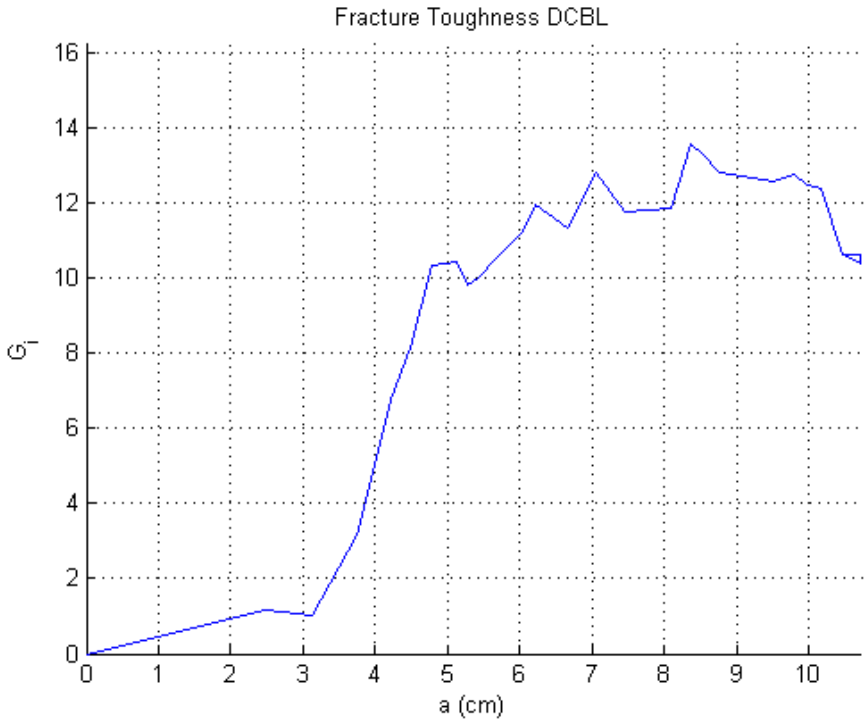

Figure 4.8: Fracture Toughness at each data point, showing the rise in fracture toughness during loading phases.

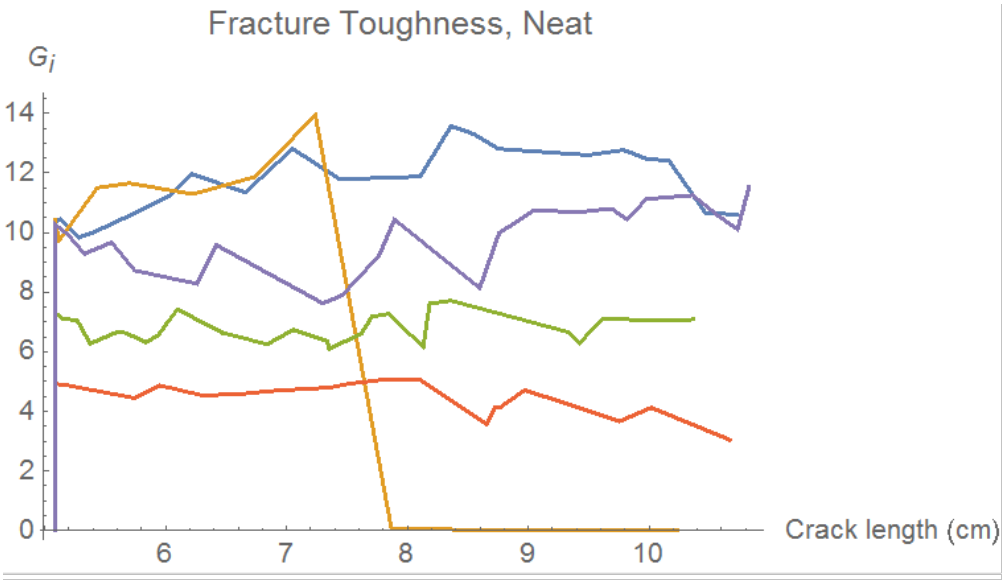

Figure 4.9: Fracture Toughness right before a release phase, showing the maximum fracture toughness for a given crack length for several neat samples.

same sample, showing only the data points right before each release phase. Figure 4.9 shows the fracture toughness of several neat samples.

A modified version of the uncertainty code was used to find the average values of the fracture toughness for several neat samples. Similar to the uncertainty code, tests that finished early were eliminated, so that the average value at a given point is computed using only tests that have not yet ended. Figure 4.10 shows the average fracture toughness for five neat samples. This code is presented in Appendix **??**

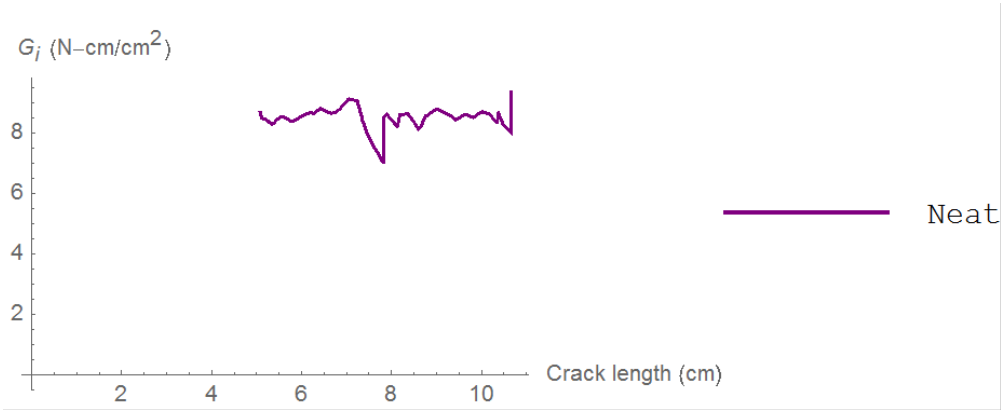

Figure 4.10: Average Fracture Toughness for neat samples.

4.4 Treated Samples

Several different treatments were applied to DCB specimens. A set of sewn samples with traditional Z-pin reinforcement was made to provide a point of comparison. Additional samples were made with three rows of injected nano-material in pin-like structures. Finally, samples were made with nano-material applied via a wet-flocking technique between each layer. The injection-control group consists of a set of samples that were injected with the needle, but without any material being added. This was to determine whether fiber displacement was affecting delamination resistance. The water-control group consisted of samples that were misted with distilled water during layup. This was to determine the effect of the water in the nano-material suspensions on the fracture toughness of the pre-preg.

4.4.1 3-row CNF injected

4.4.1.1 Characteristic Results

Next is shown the same plots for a typical sample treated with CNFs. In this sample, three rows of CNF z-pin like structures were injected using a syringe and hypodermic needle. The rows were 0.75" apart, with the first row 0.75" from the end of the Teflon pre-crack insert. The three rows were located 2.75", 3.5", and 4.25" from the beginning of the sample (the side with the pre-crack). Fig. 4.11 shows the crosshead load and crack length vs. the crosshead position.

4.4.1.2 Uncertainty

Fig. 4.12 shows load vs. crosshead position for several samples with three rows of injected CNF z-pin structures. The top graph shows the averaged values at each crosshead position along with a band showing Standard Error and Standard Deviation. The bottom graph shows data from eight 3-row samples.

4.4.1.3 Fracture Toughness

The fracture toughness for injected specimens is characterized by a flat steady-state fracture toughness until the pin rows are reached, at which point a rise in fracture toughness is observed. Figure 4.13 shows the fracture toughness for several CNF injected samples. Each curve represents a different sample. Figure 4.14 shows the averaged fracture toughness for

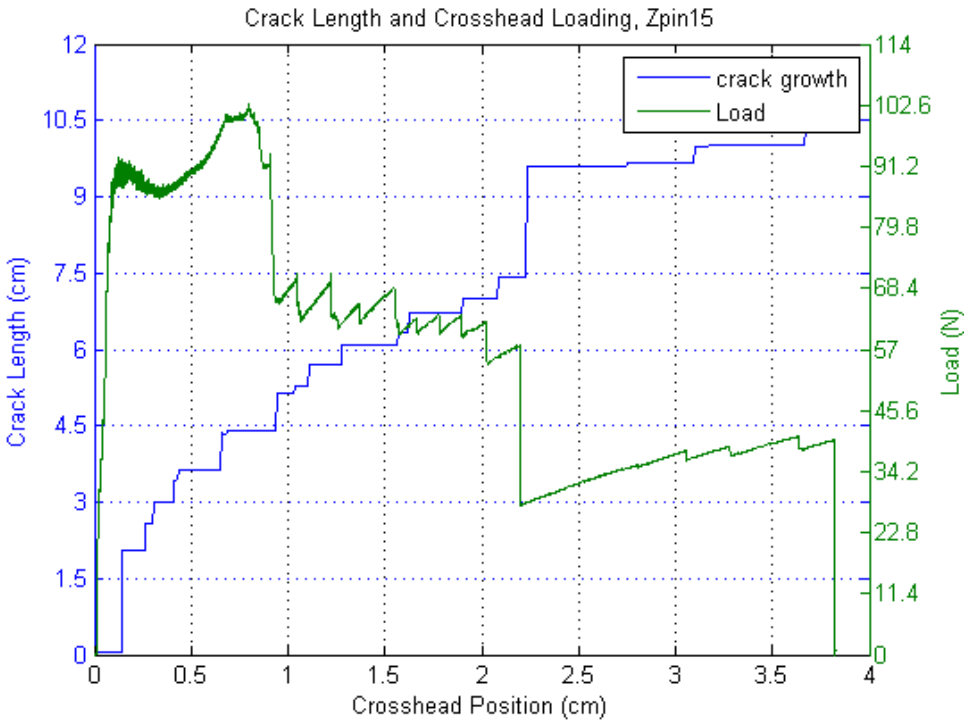

Figure 4.11: Crack length and crosshead load vs. crosshead displacement, 3-row injected CNF.

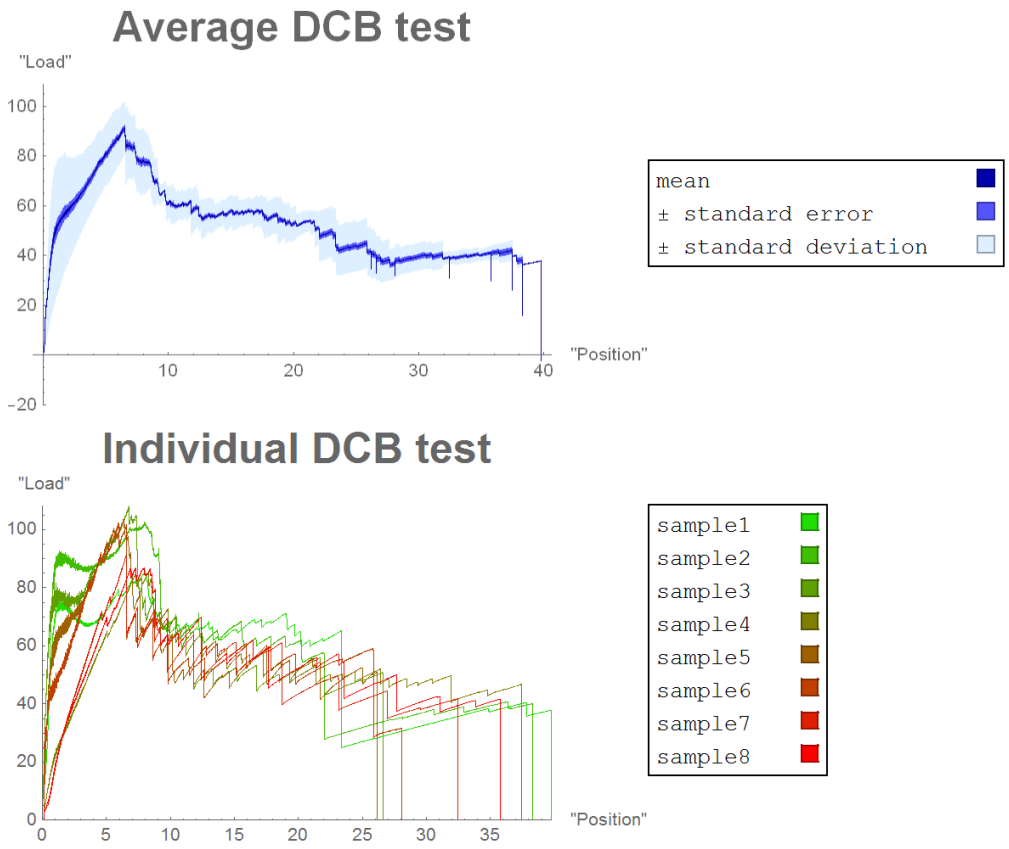

Figure 4.12: Average crosshead load vs. crosshead position, with Standard Error and Standard Deviation (top) and crosshead load vs. crosshead position for several individual DCB tests (bottom), for 3-row CNF specimens.

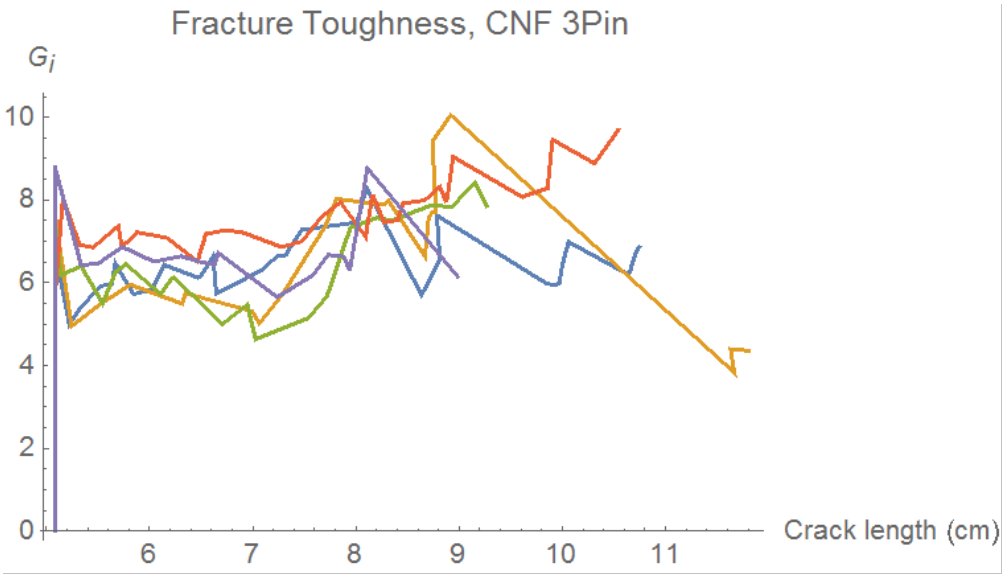

Figure 4.13: Fracture Toughness right before a release phase, showing the maximum fracture toughness for a given crack length.

each CNF injected sample.

4.4.2 3-row CNT injected

4.4.2.1 Characteristic Results

Figure 4.15 shows the crosshead load and crack length versus the crosshead displacement for a characteristic CNT injected specimen.

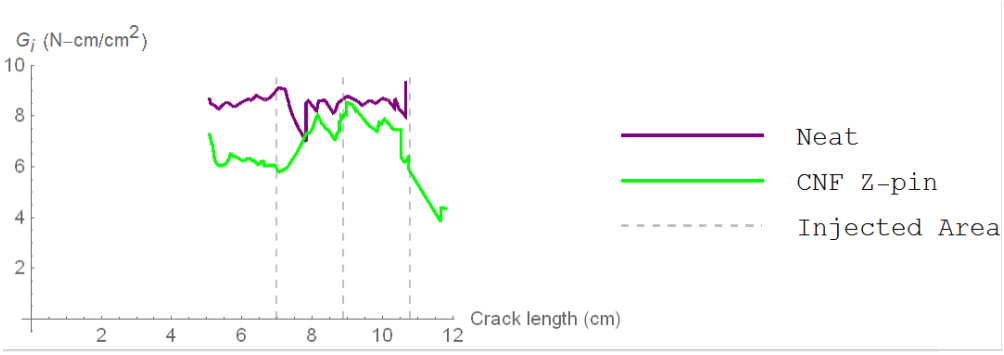

Figure 4.14: Average Fracture Toughness for 3-pin injected CNF samples, relative to neat samples.

Figure 4.15: Crack length and crosshead load vs. crosshead displacement, 3-row injected CNF.

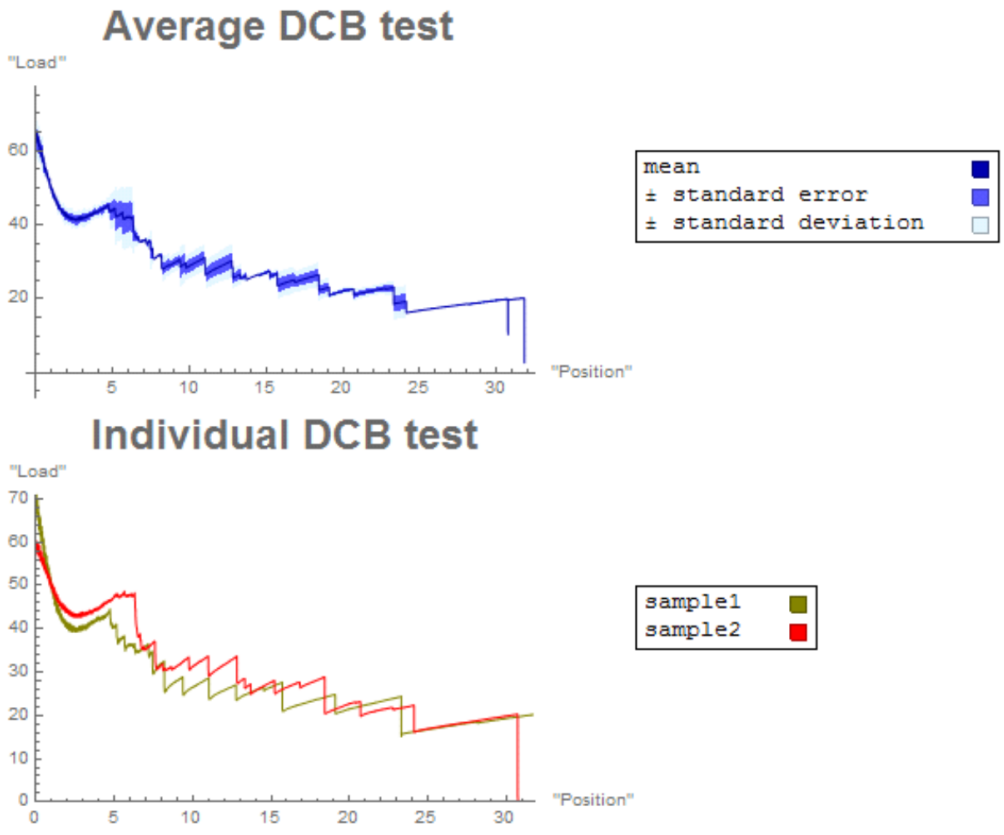

Figure 4.16: Average crosshead load vs. crosshead position, with Standard Error and Standard Deviation (top) and crosshead load vs. crosshead position for several individual DCB tests (bottom), for 3-row CNT specimens.

4.4.2.2 Uncertainty

Fig. 4.16 shows load vs. crosshead position for several samples with three rows of injected CNT z-pin like structures. The top graph shows the averaged values at each crosshead position along with a band showing Standard Error and Standard Deviation. The bottom graph shows data from two 3-row CNT samples.

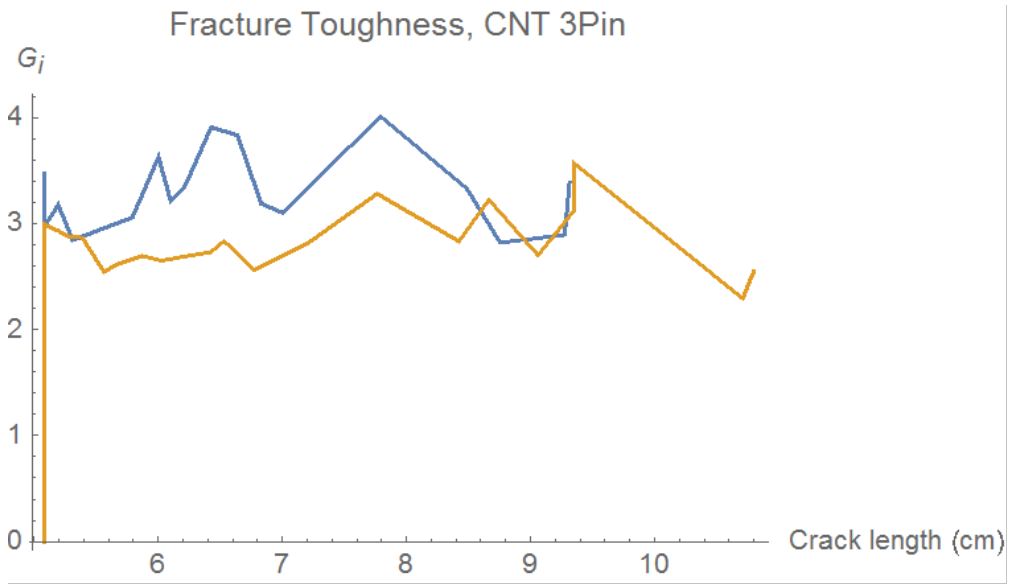

Figure 4.17: Fracture Toughness right before a release phase, showing the maximum fracture toughness for a given crack length.

4.4.2.3 Fracture Toughness

Figure 4.17 shows the fracture toughness for several CNT injected samples. Each curve represents a different sample. Figure 4.18 shows the averaged fracture toughness for each CNT injected sample.

4.4.3 CNF wet flocking

4.4.3.1 Characteristic Results

Fig. 4.19 shows the crack length and crosshead load versus crosshead displacement for a sample treated by applying CNFs using a wet-layup technique. In this case, the CNFs were

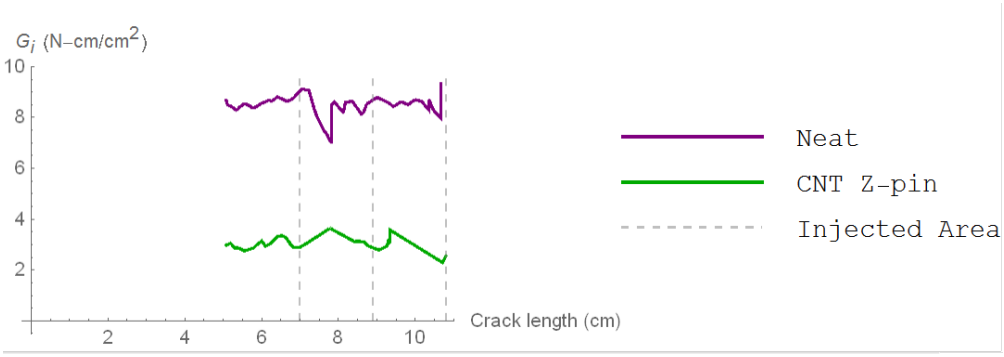

Figure 4.18: Average Fracture Toughness for 3pin CNT samples, relative to neat samples..

applied from 2.75" to 5" (beginning from the end with the pre-crack).

4.4.3.2 Uncertainty

A plot is shown for samples treated with CNF via a wet flocking technique. These samples have CNF gel spread between each layer from 2.75" to the end. Figure 4.20 shows the results for several CNF wet-flocked specimens. The top graph shows the averaged values at each crosshead position along with a band showing Standard Error one Standard Deviation. The bottom graph shows data from six wet-layup samples.

4.4.3.3 Fracture Toughness

The fracture toughness for CNF wet-flocked specimens is characterized by a sharp peak at the location where CNFs are first encountered, followed by a steady decrease. Figure 4.21 shows the fracture toughness for several CNF injected samples. Each curve represents a different sample. Figure 4.22 shows the averaged fracture toughness for each CNF injected

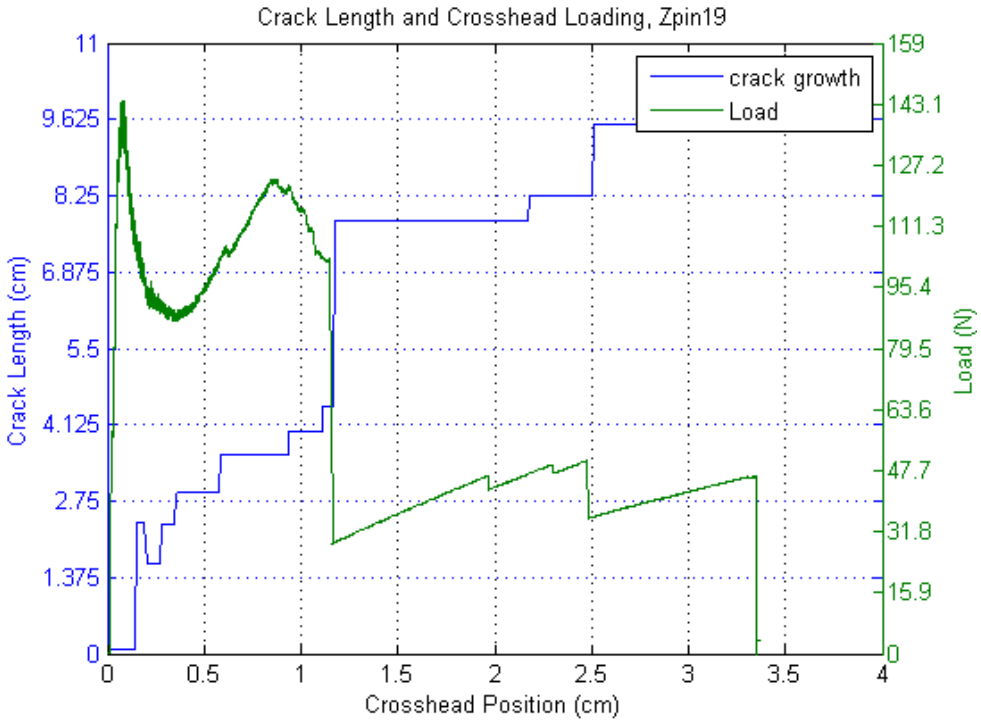

Figure 4.19: Crack length and crosshead load vs. crosshead displacement, CNF wet flocking.

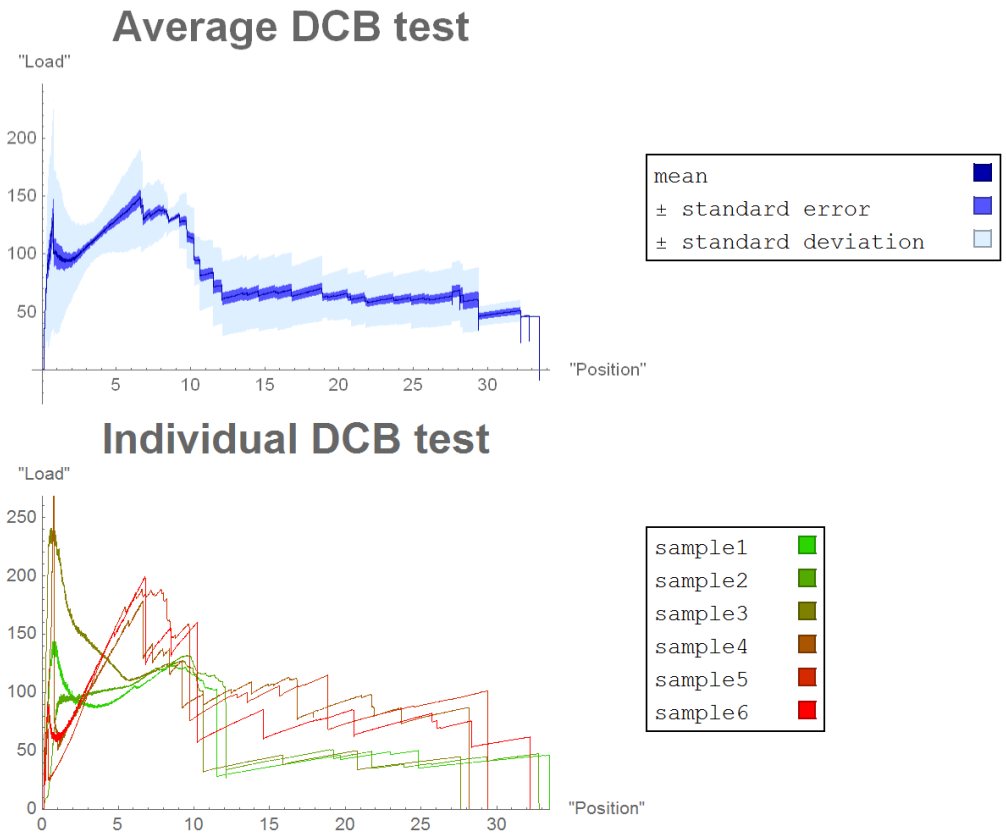

Figure 4.20: Average crosshead load vs. crosshead position, with Standard Error and Standard Deviation (top) and crosshead load vs. crosshead position for several individual DCB tests (bottom), for wet flocked CNF specimens.

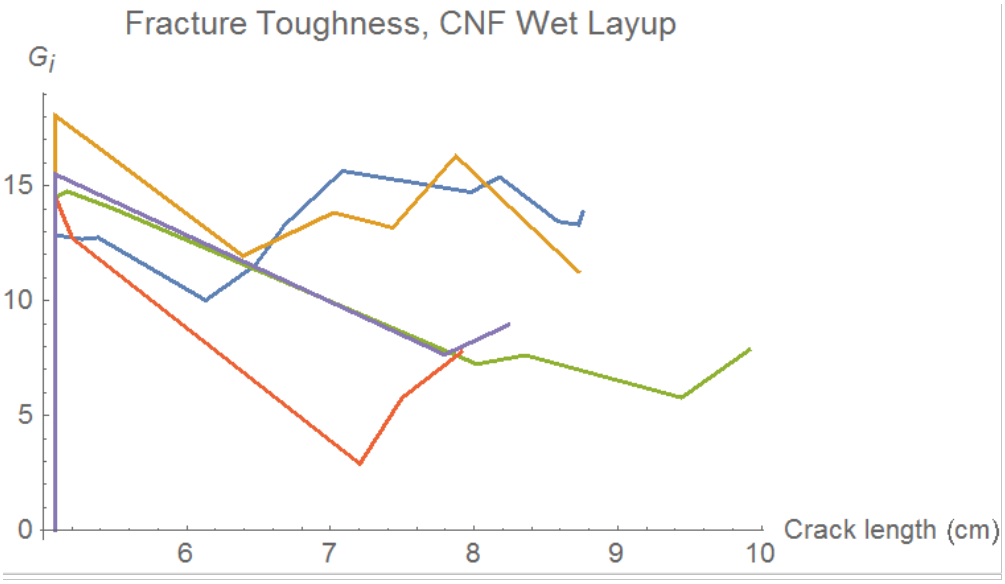

Figure 4.21: Fracture Toughness right before a release phase, showing the maximum fracture toughness for a given crack length.

sample.

4.4.4 CNT wet flocked

4.4.4.1 Characteristic Results

Fig. 4.23 shows the crack length and crosshead load vs. crosshead displacement for a sample treated by applying CNTs using a wet-layup technique. In this case, the CNTs were applied over the entire specimen.

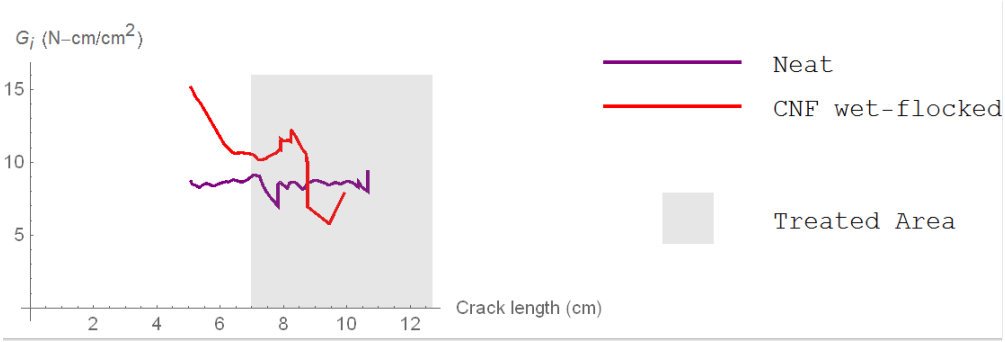

Figure 4.22: Average Fracture Toughness for CNF wet-flocked samples, relative to neat samples..

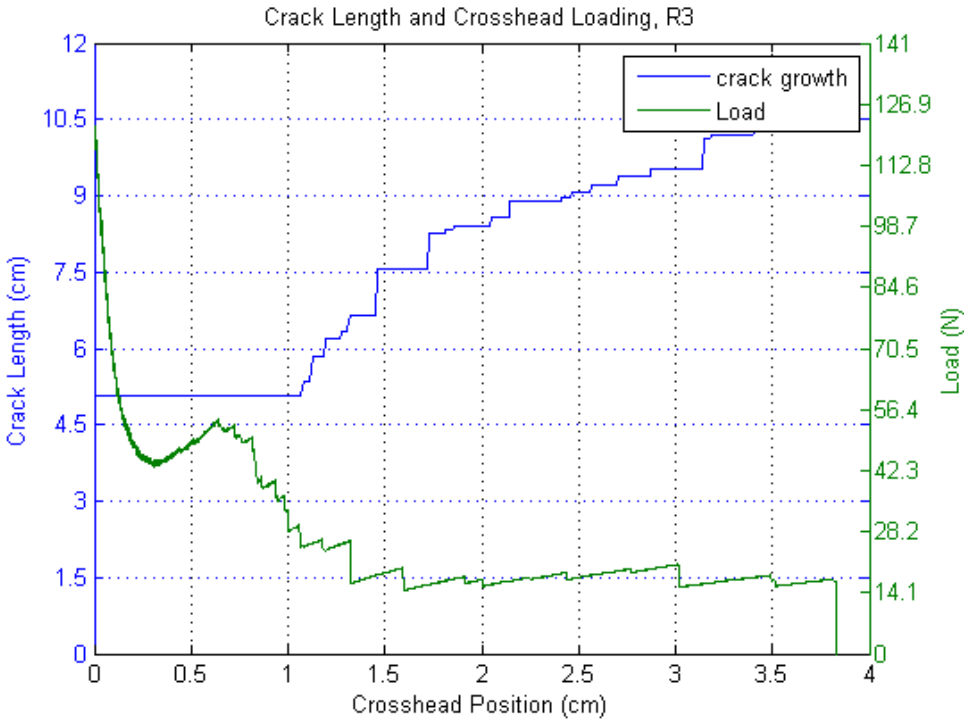

Figure 4.23: Crack length and crosshead load vs. crosshead displacement, wet flocked CNT.

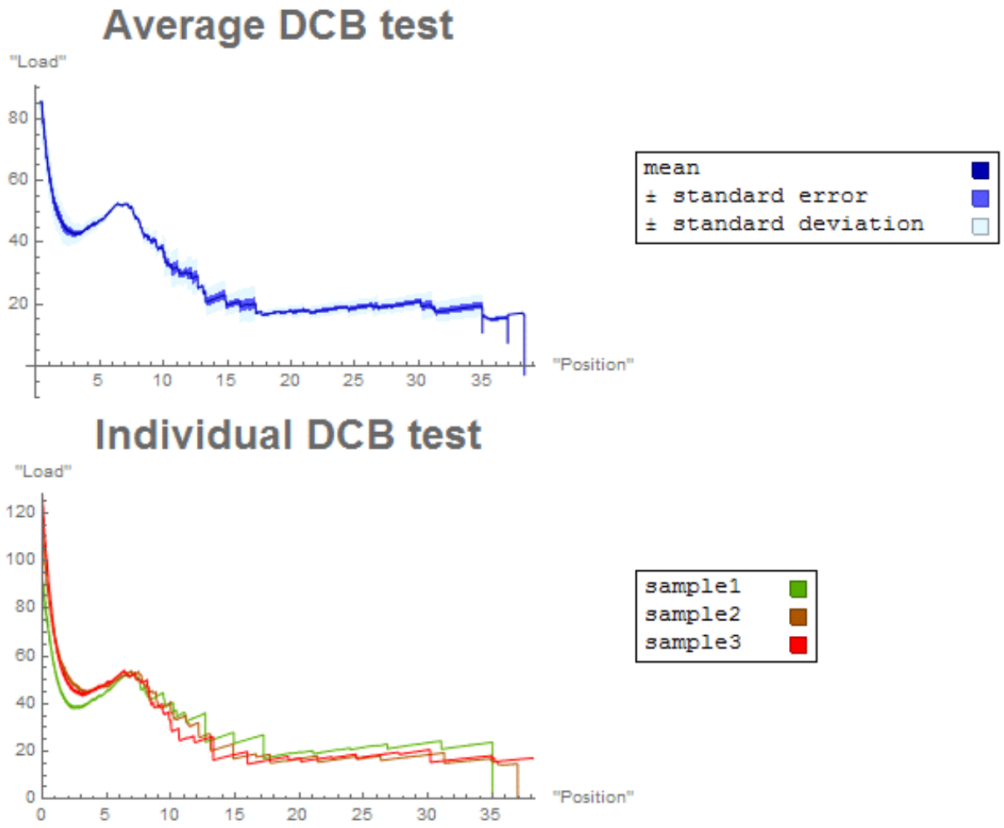

Figure 4.24: Average crosshead load vs. crosshead position, with Standard Error and Standard Deviation (top) and crosshead load vs. crosshead position for several individual DCB tests (bottom), for wet flocked CNT specimens.

4.4.4.2 Uncertainty

A plot is shown for samples treated with CNT via a wet flocking technique. These samples have CNT suspension applied between each layer from 2.75" to the end. The suspension is applied by a spray bottle, with three full sprays per layer. The top graph shows the averaged values at each crosshead position along with a band showing Standard Error one Standard Deviation. The bottom graph shows data from six wet-layup samples.

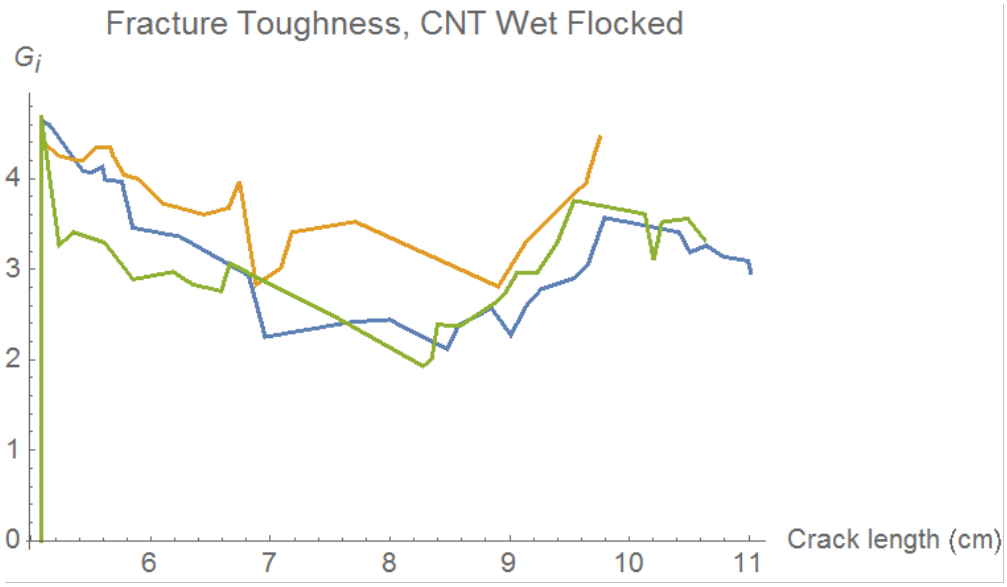

Figure 4.25: Fracture Toughness right before a release phase, showing the maximum fracture toughness for a given crack length.

4.4.4.3 Fracture Toughness

The fracture toughness of CNT wet-flocked specimens is characterized by a decrease in fracture toughness over the treated region. Figure 4.25 shows the fracture toughness for several CNT injected samples. Each curve represents a different sample. Figure 4.26 shows the averaged fracture toughness for each CNT injected sample.

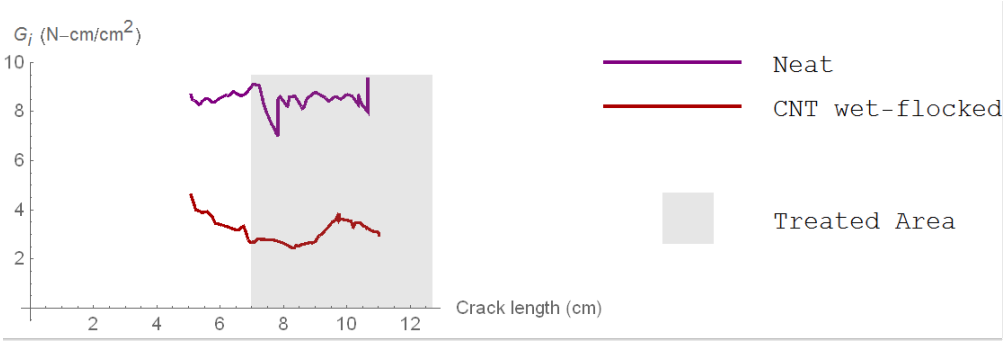

Figure 4.26: Average Fracture Toughness for wet-flocked CNT samples, relative to neat samples.

4.4.5 Injection-Control Group

4.4.5.1 Characteristic Results

The injection-control group was made to observe the effects of fiber displacement separately from that of the CNF pin-like injected structures. Fig. 4.27 shows the crack length and crosshead load vs. crosshead displacement for a sample treated by puncturing the material with an awl, but without adding any nano-material.

4.4.5.2 Uncertainty

A plot is shown for the control group. Holes were made in the samples along three rows in the same manner as the injected specimens, but no CNF or CNT material was added. The top graph shows the averaged values at each crosshead position along with a band showing Standard Error one Standard Deviation. The bottom graph shows data from six wet-layup

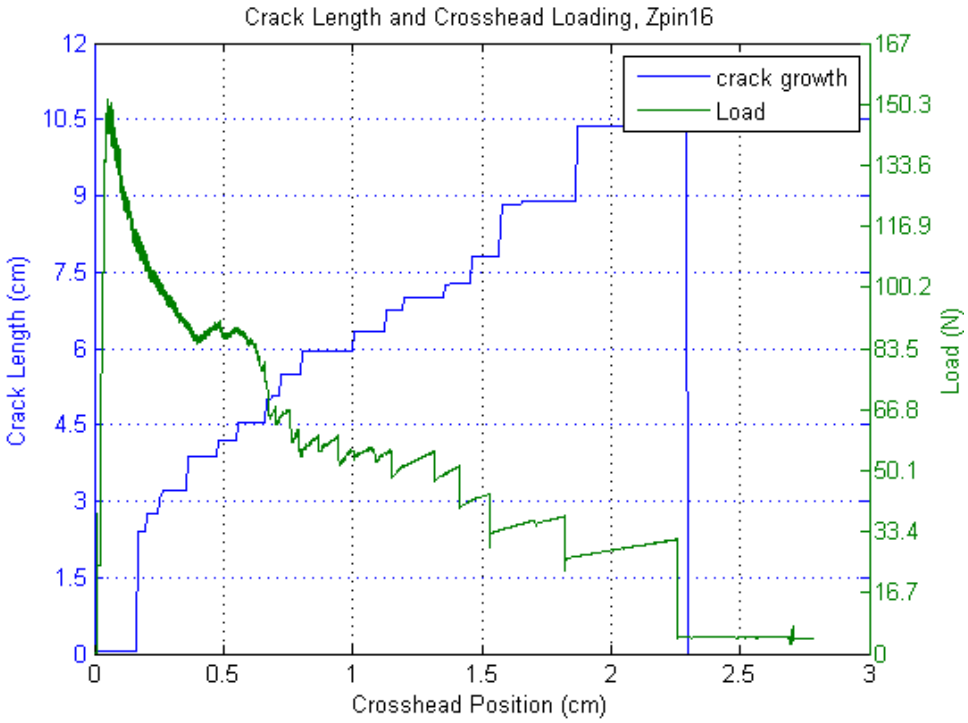

Figure 4.27: Crack length and crosshead load vs. crosshead displacement, CNF wet flocking.

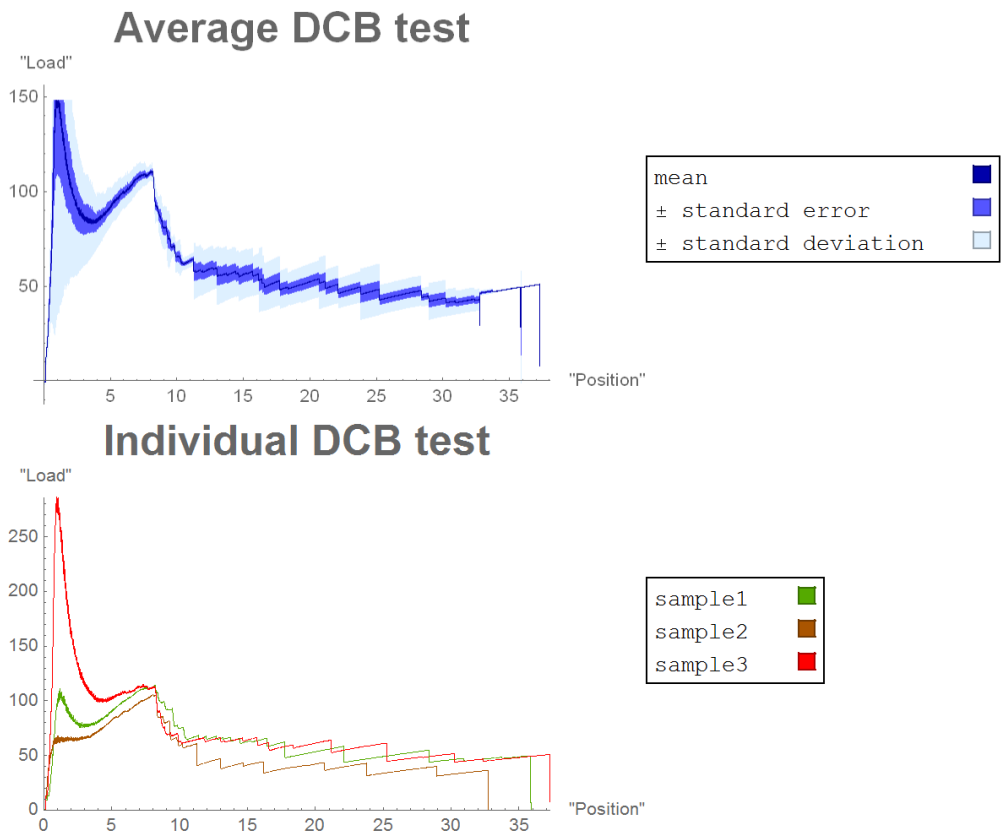

Figure 4.28: Average crosshead load vs. crosshead position, with Standard Error and Standard Deviation (top) and crosshead load vs. crosshead position for several individual DCB tests (bottom), for injection-control specimens.

samples. Figure 4.28 shows the results for several injection-control specimens. The top graph shows the averaged values at each crosshead position along with a band showing Standard Error one Standard Deviation. The bottom graph shows data from three injection-control samples.

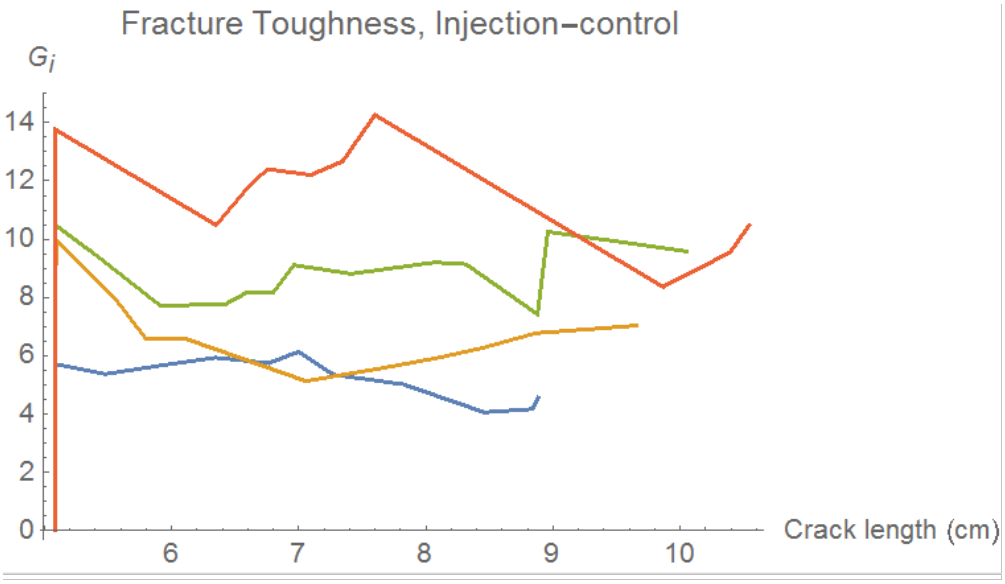

Figure 4.29: Fracture Toughness right before a release phase, showing the maximum fracture toughness for a given crack length.

4.4.5.3 Fracture Toughness

The fracture toughness of the control group is characterized by a decrease in fracture toughness over the treated region. Figure 4.29 shows the fracture toughness for several injection-control samples. Each curve represents a different sample. Figure 4.30 shows the averaged fracture toughness for each injection-control sample.

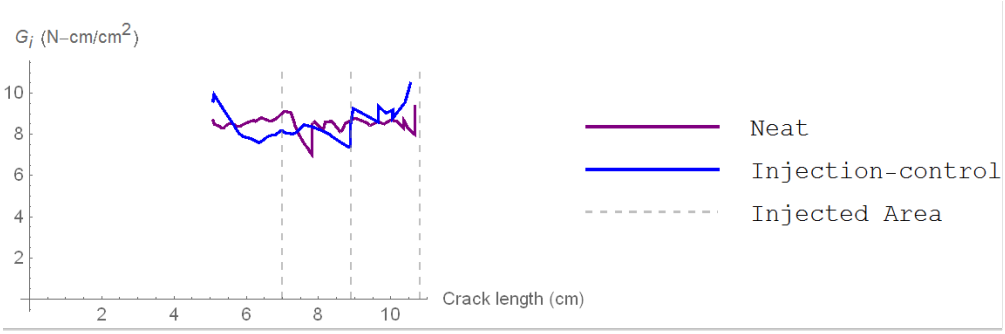

Figure 4.30: Average Fracture Toughness for injection-control samples, relative to neat samples.

4.4.6 Water-Control Group

4.4.6.1 Characteristic Results

The water-control group was made to observe the effects of the water in the CNF gel and CNT suspension.

4.4.6.2 Uncertainty

A plot is shown for the control group. Water was added to the specimens using a spray bottle. The top graph shows the averaged values at each crosshead position along with a band showing Standard Error one Standard Deviation. The bottom graph shows data from six wet-layup samples. Figure 4.32 shows the results for several water-control specimens. The top graph shows the averaged values at each crosshead position along with a band showing Standard Error one Standard Deviation. The bottom graph shows data from six water-control samples.

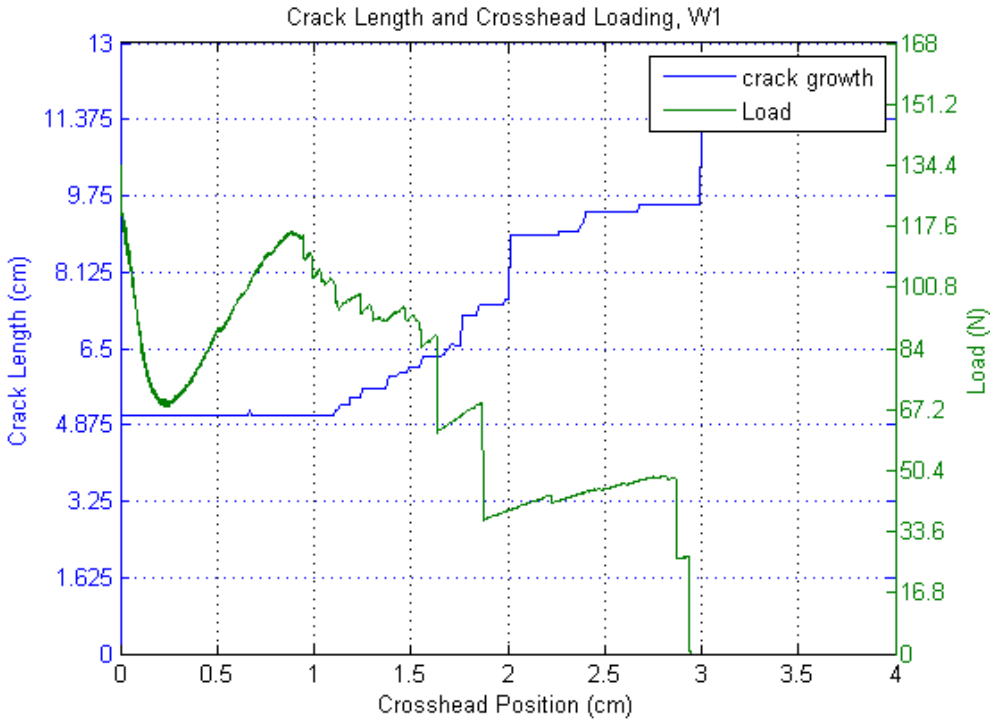

Figure 4.31: Crack length and crosshead load vs. crosshead displacement, Water Control.

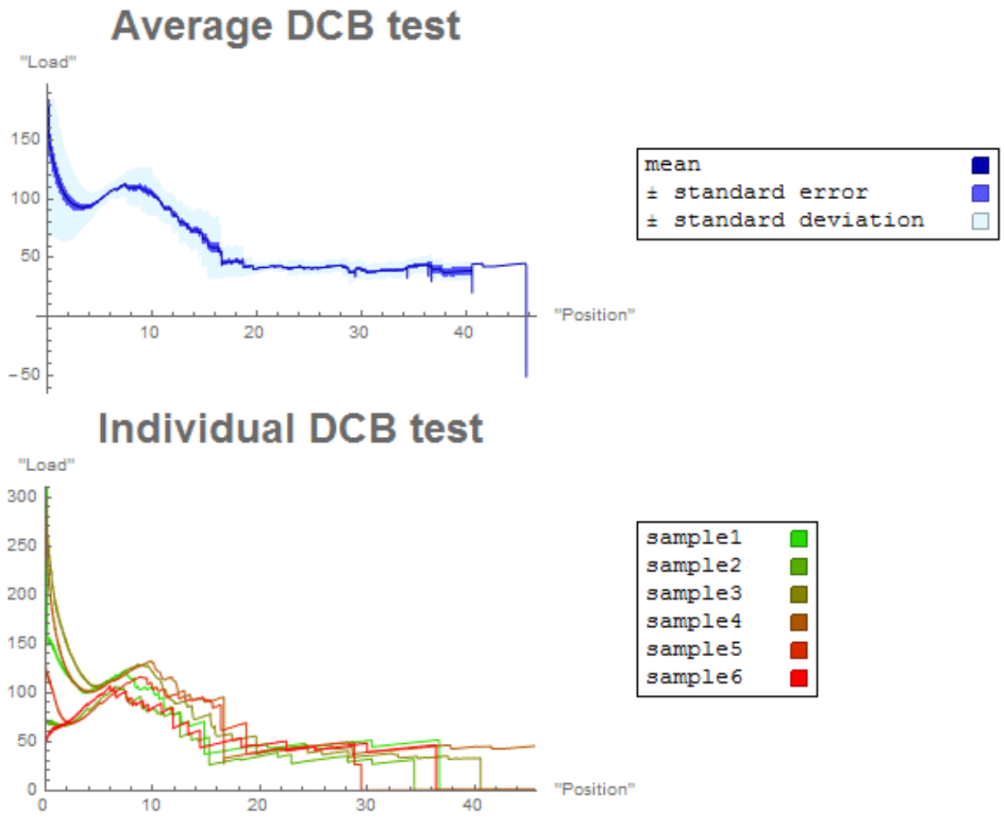

Figure 4.32: Average crosshead load vs. crosshead position, with Standard Error and Standard Deviation (top) and crosshead load vs. crosshead position for several individual DCB tests (bottom), for water-control specimens.

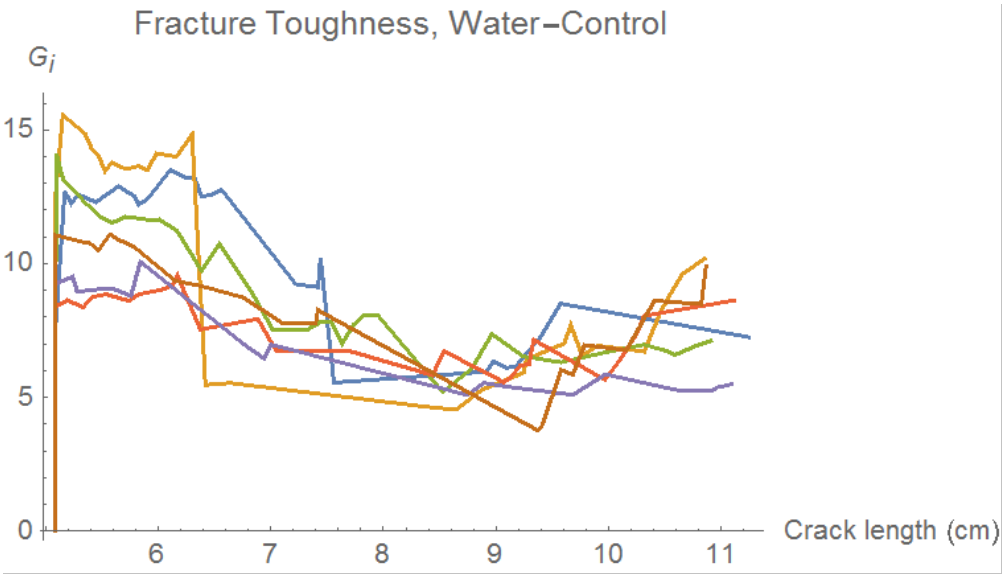

Figure 4.33: Fracture Toughness right before a release phase, showing the maximum fracture toughness for a given crack length.

4.4.6.3 Fracture Toughness

The fracture toughness of the control group is characterized by a decrease in fracture toughness over the treated region. Figure 4.33 shows the fracture toughness for several water-control samples. Each curve represents a different sample. Figure 4.34 shows the averaged fracture toughness for each water-control sample.

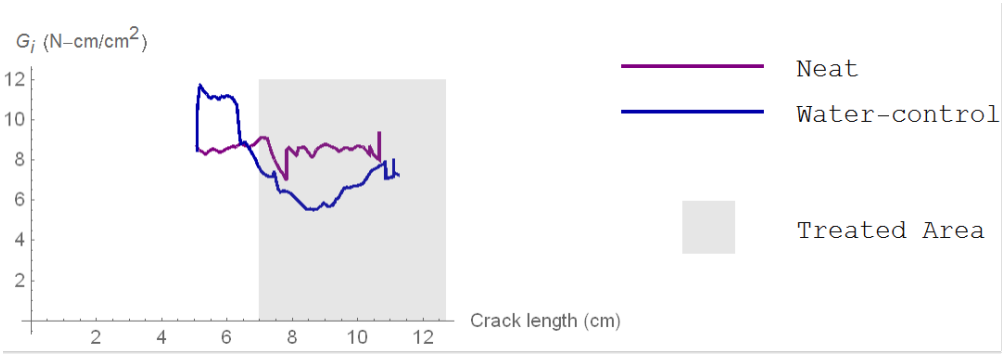

Figure 4.34: Average Fracture Toughness for water-control samples, relative to neat samples.

4.4.7 sewn

4.4.7.1 Characteristic Results

For comparison, a sample set was made using traditional z-pins. A layup of 20 layers of pre-preg was made, and then carbon fiber thread was sewn through the thickness of the sample in three rows. The rows were located at 2.75", 3.5", and 4.25" from the end with the pre-crack. When tested, these sample showed considerably larger peaks in the loading phase when a row of stitched z-pins was reached. The crosshead load increased significantly prior to failure of the z-pins. When the pins did fail, sufficient strain energy had built up to suddenly and violently delaminate the remainder of the sample. The samples broke after failure of either the first or second row of pins.

As seen in fig. 4.35, the first row of pins held at 6.7 cm (2.66") while the crosshead load rose to a peak value of 225 N. The first row on pins then ruptures, and the crack advanced immediately to the next row at 8.47 cm (3.33"). This row of pins held until the crosshead

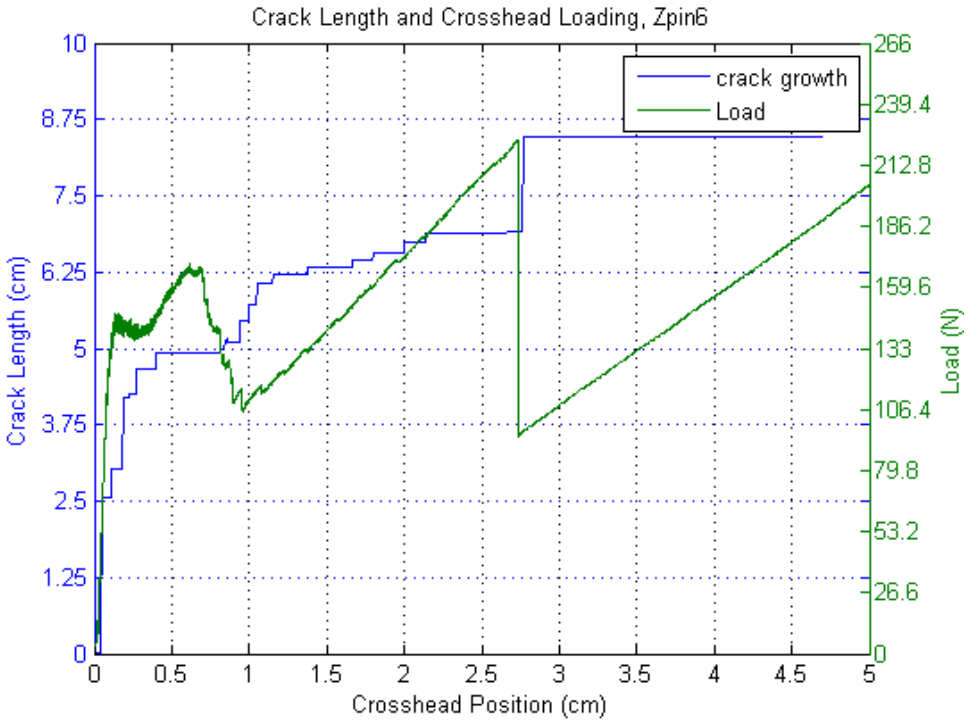

Figure 4.35: Crack length and crosshead load vs. crosshead displacement, carbon fiber z-pin.

load reached about 192 N, when the sample failed completely.

4.4.7.2 Uncertainty

Figure 4.36 shows a plot of crosshead load vs. crosshead position for two sewn sample tests. The top graph shows a plot of the averaged values at each crosshead position and a band showing Standard Error and a band showing one standard deviation from the average. The bottom graph shows data for two sewn samples.

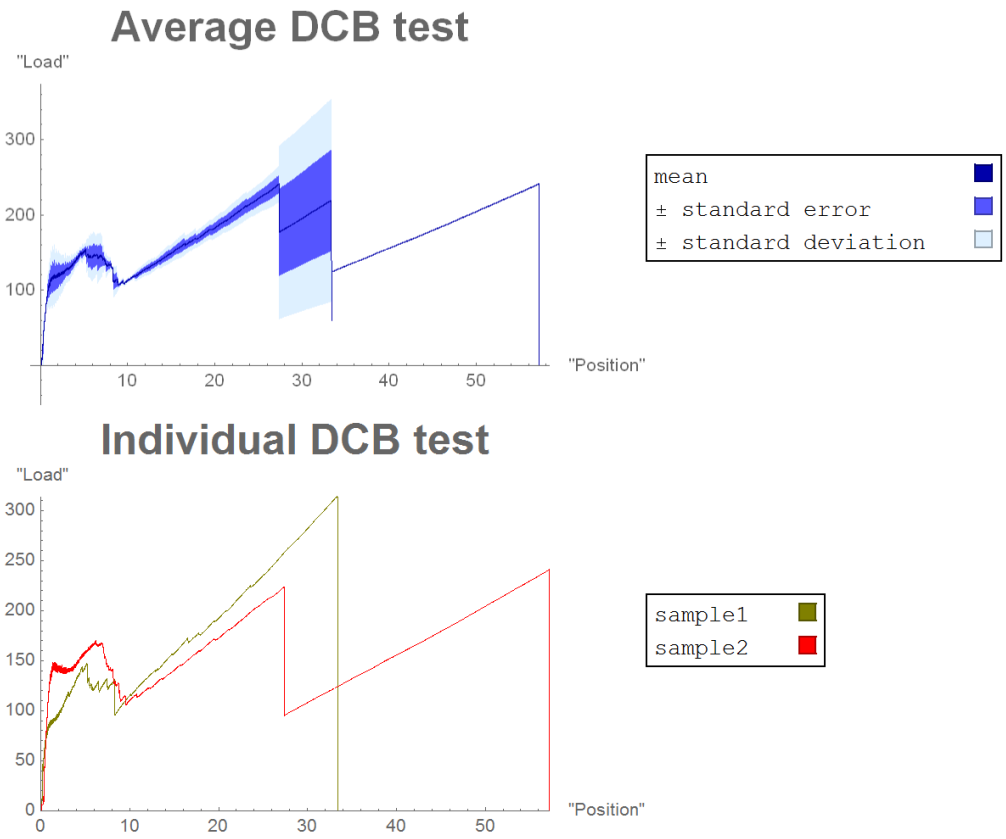

Figure 4.36: Average crosshead load vs. crosshead position, with Standard Error and Standard Deviation (top) and crosshead load vs. crosshead position for several individual DCB tests (bottom), for carbon fiber z-pin specimens.

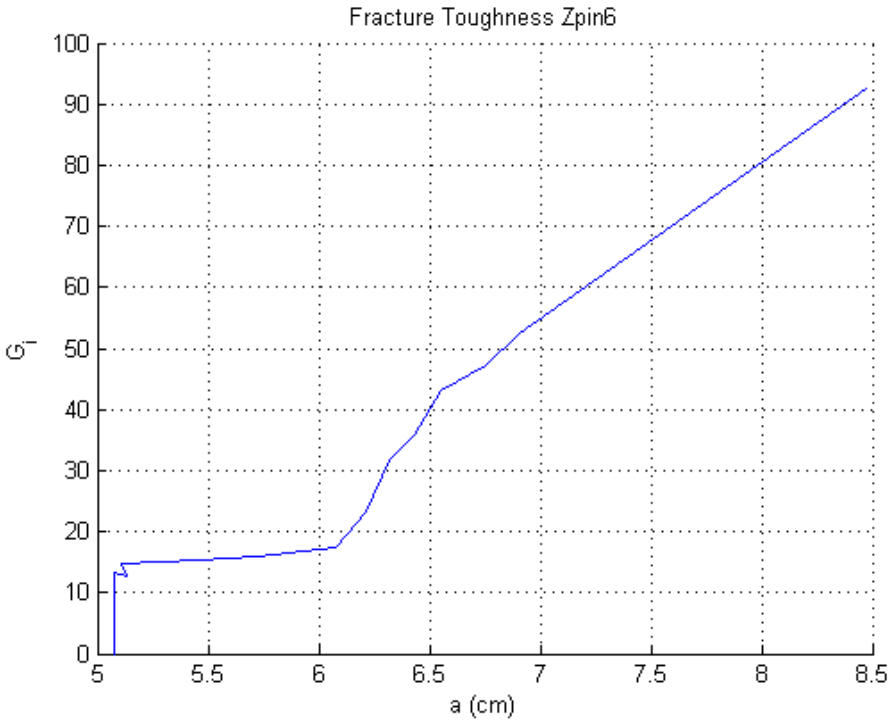

Figure 4.37: Fracture Toughness right before a release phase, showing the maximum fracture toughness for a given crack length.

4.4.7.3 Fracture Toughness

The fracture toughness for a characteristic sewn sample is shown in fig. 4.37. The fracture toughness of sewn samples is characterized by a sharp rise in fracture toughness when the z-pin is reached.

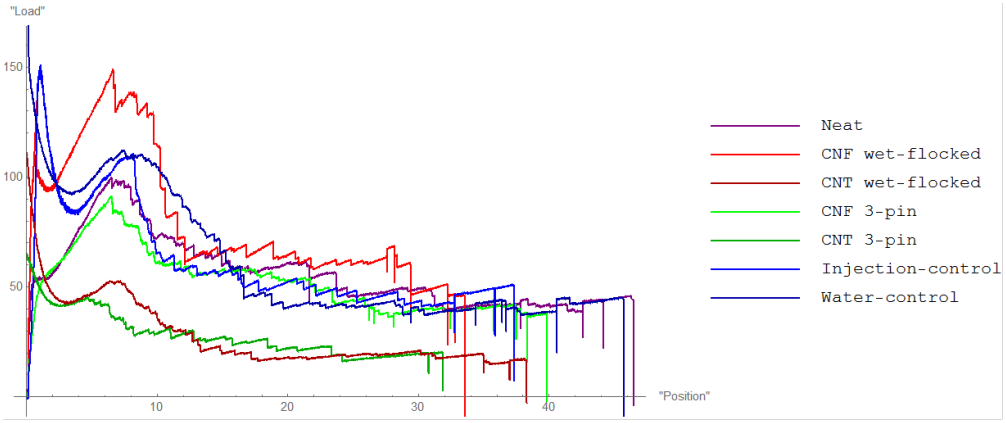

Figure 4.38: Averaged crosshead load vs. crosshead position curves, showing neat, CNF injected, CNT injected, CNF wet-flocked, CNT wet-flocked, and injection-control sample types.

4.4.8 Comparison with Neat Samples

Using these averaged plots, a comparison can be made between each treated sample type and neat (untreated) samples.

The averaged crosshead load from all the above cases are shown in fig. 4.38. Fig. 4.39 shows the averaged fracture toughness curves for each sample type.

4.5 SEM Microscopy

The fracture surface was examined under a scanning electron microscope. A Jeol JCM-5000 Benchtop SEM was used to inspect the surface.

Rectangular pieces of the fractured DCB specimen were cut using a bandsaw. The pieces

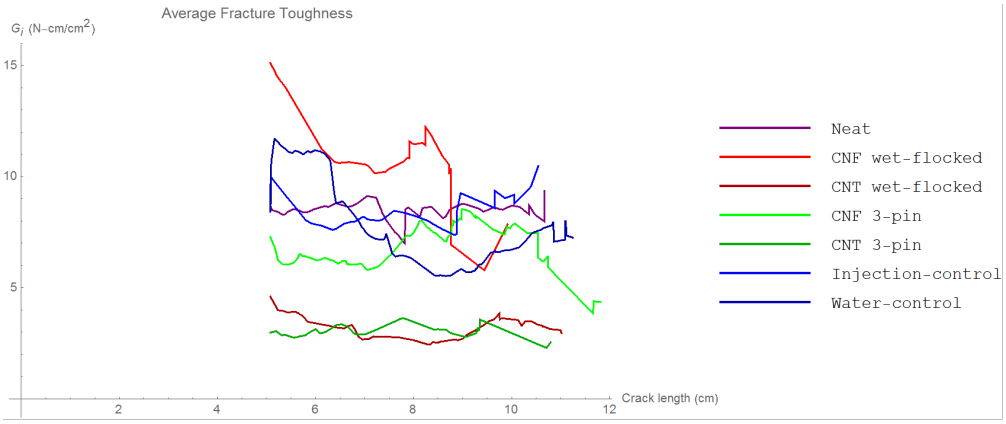

Figure 4.39: Average Fracture Toughness vs. crack length, showing neat, CNF injected, CNT injected, CNF wet-flocked, CNT wet-flocked, and injection-control sample types.

measured approximately 1"x0.25". They were cut to this size so that they could fit in the SEM microscope. The cuts were aligned so that the treated section of the DCB coupons would be positioned in the center of the SEM specimen. Figure 4.40 shows the location from which the SEM specimens were taken.

The SEM specimens were sputtered with gold wire for 15 seconds to improve image quality. This increased the specimen's conductance and reduced charge buildup which was found to adversely effect the image clarity. Images were taken for each specimen type. Below are presented images for several sample types. The results of the test were inconclusive, as no discernible difference could be observed in the crack surface, and no nano-particles could be observed.

Figure 4.41 shows two SEM images of the fracture surface of a neat (untreated) DCB specimen. The left-hand side is a low magnification image showing individual fiber squares, and

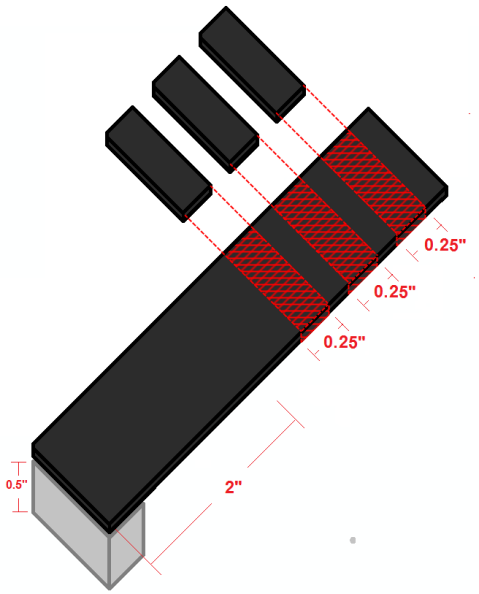

Figure 4.40: Schematic showing area of DCB coupons analysed under the SEM microscope.

the right-hand side is a medium magnification showing individual fibers. Likewise, figure 4.42 shows similar images for a wet-flocked CNF image. Figure 4.43 shows a wet-flocked CNT sample, figure 4.44 shows a 3-pin CNF samples, and figure 4.45 shows the same images for an injection-control specimen.

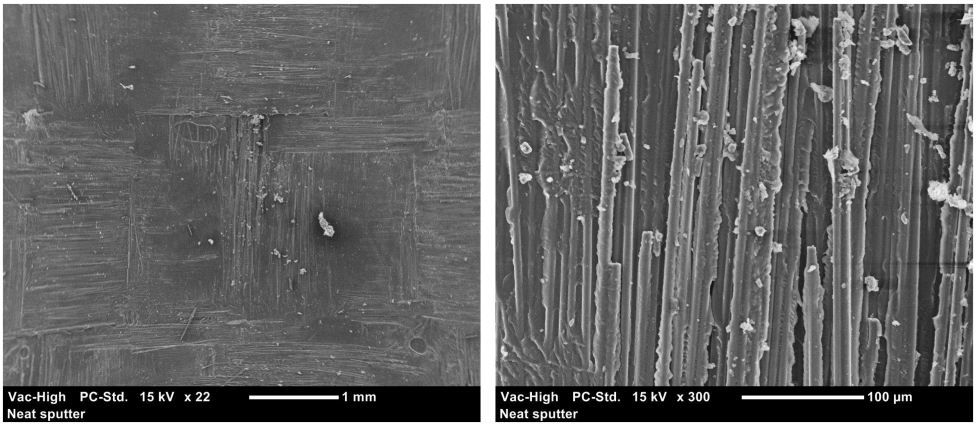

Figure 4.41: SEM images of the fracture surface of a neat DCB specimen after testing.

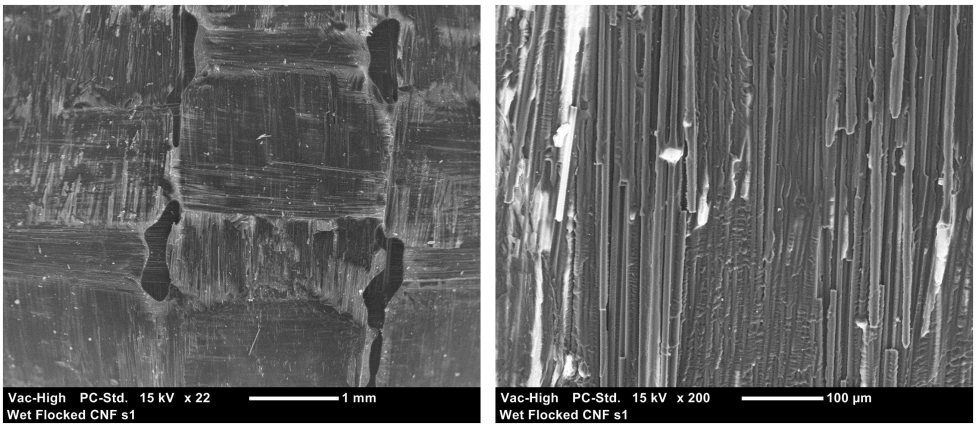

Figure 4.42: SEM images of the fracture surface of a wet-flocked CNF specimen after testing.

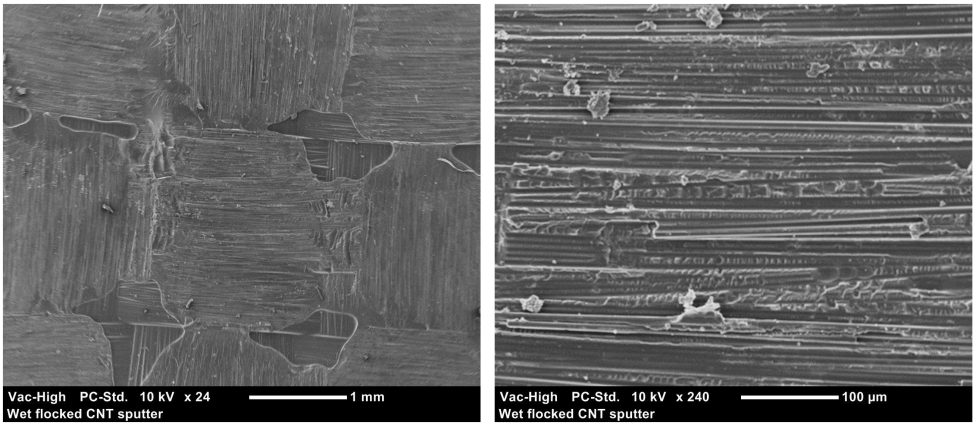

Figure 4.43: SEM images of the fracture surface of a wet-flocked CNT specimen after testing.

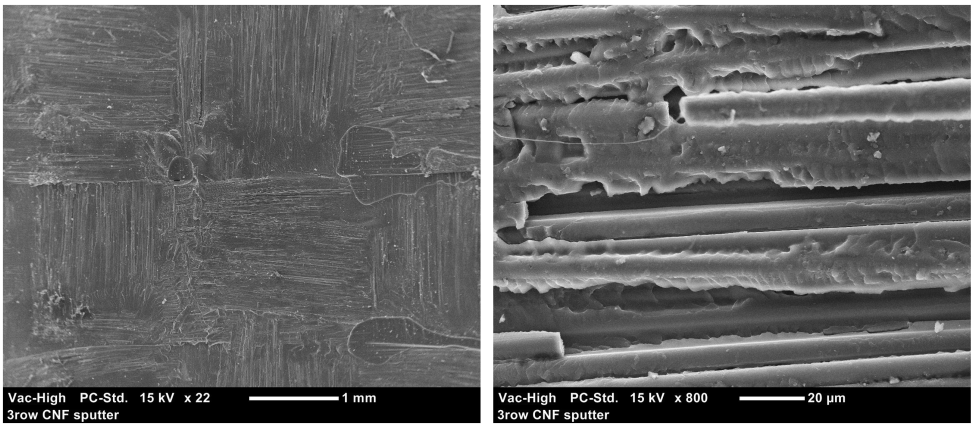

Figure 4.44: SEM images of the fracture surface of a neat DCB specimen after testing.

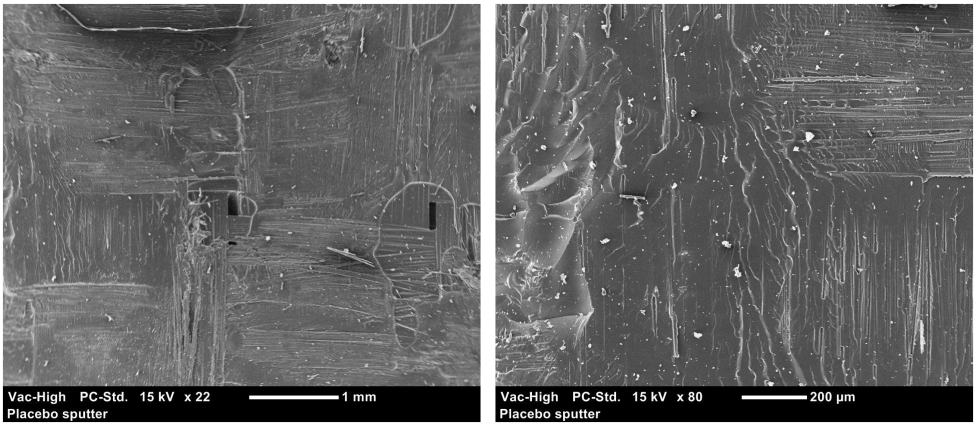

Figure 4.45: SEM images of the fracture surface of a neat DCB specimen after testing.

Chapter 5

Discussion

The results of the stitched samples matched the expected result for a traditional z-pinned or stitched DCB coupon. Ranatunga and Clay[18] compared neat DCB coupons with z-pinned DCB coupons, experimentally. They found that the reinforced sample's exhibited a steady increase in fracture toughness until a maximum value was reached, after which the fracture toughness remained relatively constant. The stitched sample in this work exhibited a similar rise in fracture toughness, but did not reach a steady value. After the peak fracture toughness was reached, the stitched sample fully delaminated and the test ended. This difference is likely due to the difference in the nature of the through-thickness reinforcement. Ranatunga and Clay used several dozen rows of z-pins, whereas the stitched specimens in this work had only three rows. Once the sample had built up sufficient strain energy to break the first or second row, the samples in this work fully delaminated the rest of the way. This contrasts with the higher number of rows in Ranatunga and Clay's specimens which allowed them to

reached a steady state. The higher number of z-pins increased the likelihood that the crack would be arrested by a z-pin row.

Treatment of CFRP with nano-materials to improve fracture toughness is a subject of significant interest, and much research has been done in the area. In this work, a novel method for introducing nano-materials was considered. The effect of injecting particles in an aqueous suspension, using a hypodermic needle, into pre-preg CFRP fabric prior to cure, was experimentally determined using a Mode 1 delamination test. The effect of introducing nano-particales by wet flocking, as demonstrated by Karwa et al. [7], was also examined. In both cases, the fracture toughness was compared to that of neat (untreated) samples. Additionally, the effect of using a needle to make holes in carbon fiber pre-preg fabric (without introducing any additives) was examined, in order to determine whether fiber displacement caused by inserting a needle into the fabric would alter the specimen's fracture toughness.

The injection of both CNF and CNT nano-materials into the CFRP was not found to provide an increase in fracture toughness. Figure 4.14 shows the average fracture toughness for CNF injected samples, and figure 4.18 shows the average fracture toughness for CNT injected samples. The injected material was expected to act like traditional z-pins and provide through-thickness strength, but this strength was not observed. In the case of injected CNF specimens, there was an increase in the fracture toughness through the treated region, relative to the untreated portion of the specimen, but, even through the treated area, the injected CNF specimen's fracture toughness was less than that of a neat sample, as shown in figure 4.39.

The fracture toughness of the injection-control group was nominally the same as that of the neat samples, although a slight decrease was observed through the treated region. Figure 4.30 shows the average fracture toughness for injection-control samples. This decrease, relative to neat samples, suggests that fiber displacement may have been partly responsible for the decrease in fracture toughness observed in all specimens which were injected.

The wet-flocked specimens did exhibit an increase in fracture toughness, relative to the untreated samples, as shown in figure 4.39. Based on this increase we can conclude that CNFs are capable of improving delamination resistance in CFRPs, relative to untreated specimens.

The CNFs used in this work were suspended in distilled water. As the water evaporated during cure, minimal cross-linking was likely able to occur between cellulose chains. If this is the case, then it severely limited the ability of the CNFs to act like a rigid z-pin. The injected specimens failed to provide enhanced performance. It is theorized that he CNFs did not form a rigid matrix in the injection hole, and so were not concentrated in such a way as to provide an increase in fracture resistance. The wet-flocked specimens, on the other hand, did demonstrate increase performance. It is theorized that since the CNFs were concentrated at the laminar boundaries, they were able to provide an increase in fracture resistance by forming a rigid matrix to resist delamination. The CNFs mixed with the epoxy to provide enhanced inter-laminar bonding.

The specimens treated with CNTs consistently performed very poorly. The CNTs used in this work were not of very high quality, being between 40-60 percent carbon, by weight. They

also were not functionalized, which likely prevented them from forming a good dispersion during ultrasonification, as well as during epoxy cure. Functionalized CNTs demonstrate significantly better solubility in most mediums, including water [29, 30, 31]. Pristine (unmodified) CNTs tend to cohere when dissolved in water due to high surface area and lack of chemical affinity with water [32]. Inspection of the CNT dispersion, prior to being injected or sprayed onto the pre-preg, showed visible clumping of CNTs, as well as observable precipitation of CNTs within the container, during the layup process.

The results of the SEM analysis were inconclusive, as no nano-particles were observed in the fractured DCB specimens. It is possible that the nano-material did not remain where it was originally added, but partially flowed through the sample during cure. Epoxy squeeze-out was observed along the edges of the CFRP plates when they were removed from the press, which suggests that nano-material may have traveled with the epoxy and ended up in another part of the sample then intended. Since the particles were not observed under the microscope, this cannot be verified, however it should be considered as a possible explanation of the results. Specifically, it can be observed in figure 4.39 that the untreated sections of DCB samples do not match the corresponding sections of the neat samples. Ideally, the untreated sections ought to behave the same as neat samples. This discrepency could be the result of CNF or CNT flow during cure.

Chapter 6

Conclusion

The water-control group demonstrated experimentally that water present in CFRP pre-preg may reduce the fracture toughness of the material. This suggests that aqueous suspensions of nano-particles in CFRP pre-preg may have adverse effects on the material's properties, due to the presence of water during cure.

The injection-control group demonstrated experimentally that fiber dislocation in CFRP pre-preg may have adverse effects on the material's mechanical properties, and may reduce inter laminar bonding.

Injection of CNFs via a hypodermic needle does not appear to provide enhanced mechanical properties, and may even cause reduced fracture toughness in CFRPs. This reduction may be due to fiber dislocation during the injection process, as well as the presence of water, from the CNF suspension, during cure. Additional research focusing on methods of evaporating

the water from the CNFs, as well as increasing the weight percentage of CNFs injected into the pin-like structures could improve results, but fiber dislocation is inherent to this method and appears to cause adverse effects in the material. A solvent exchange, replacing the water in the CNF gel with another solvent could improve results.

Wet-flocking of CNFs in pre-preg does appear to provide some increase in fracture toughness. Wet-flocked CNFs were shown experimentally in this work to be able to improve fracture toughness of CFRP pre-preg. This technique is relatively simple and does not adversely effect the fabric weave by dislocation of fibers. Wet-flocking of CNFs, then, may be able to provide beneficial mechanical improvement to CFRP components being used in structural elements.

The application of pristine CNTs appears to adversely effect CFRP pre-preg, and was shown experimentally in this work to reduce fracture toughness when applied by injection and wet-flocking in an aqueous medium. Addtional research focusing on improving the CNT dispersion, evaporating the water prior to cure, suspending the CNTs in a different medium, and using functionalized CNTs may provide improved results.

Bibliography

[1] D. Sadava, D. M. Hillis, H. C. Heller, and M. Berenbaum, *Life: The Science of Biology*. Sinauer Associates, 2014.

[2] I. Sir and D. Plackett, "Microfibrillated cellulose and new nanocomposite materials: a review," *Cellulose*, vol. 17, pp. 459–494, 21 February 2010.

[3] A. Mouritz, "Review of z-pinned composite laminates," *Composites Part A: Applied Science and Manufacturing*, vol. 38, p. 23832397, 2007.

[4] K. Dransfield and C. Baillie, "Improving the delamination resistance of cfrp by stitchinga review," *Composites Science and Technology*, vol. 50, p. 305317, 1994.

[5] A. Mouritz, M. Bannister, P. Falzon, and K. Leong, "Review of applications for advanced three-dimensional fibre textile composites," *Composites Part A: Applied Science and Manufacturing*, vol. 30, p. 14451461, 1999.

[6] L. Tong, A. Mouritz, and M. Bannister, *3D Fibre Reinforced Polymer Composites*. Elsevier Science, 2002.

[7] A. N. Karwa, T. J. Barron, V. A. Davis, and B. J. Tatarchuk, "A novel nano-nonwoven fabric with three-dimensionally dispersed nanofibers: Entrapment of carbon nanofibers within nonwovens using the wet-lay process," *Nanotechnology*, vol. 23, p. 185601, 2012.

[8] F. H. Gojny, M. H. Wichmann, B. Fiedler, W. Bauhofer, and K. Schulte, "Influence of nano-modification on the mechanical and electrical properties of conventional fibre-reinforced composites," *Composites Part A: Applied Science and Manufacturing*, vol. 36, p. 15251535, 2005.

[9] E. T. Thostenson and Z. Ren, "Advances in the science and technology of carbon nanotubes and their composites: a review," *Composites Science and Technology*, vol. 61, p. 18991912, 2001.

[10] A. Warrier, A. Godara, O. Rochez, L. Mezzo, F. Luizi, L. Gorbatikh, S. V. Lomov, A. W. VanVuure, and I. Verpoest, "The effect of adding carbon nanotubes to glass/epoxy composites in the fibre sizing and/or the matrix," *Composites Part A: Applied Science and Manufacturing*, vol. 41, p. 532538, 2010.

[11] "Standard test method for mode i interlaminar fracture toughness of unidirectional fiber-reinforced polymer matrix composites1," *ASTM International, West Conshohocken, PA*, 2009.

[12] P. Robinson and D. Song, "A modified dcb specimen for mode i testing of multidirectional laminates," *Journal of Composite Materials*, vol. 26, pp. 1554–1557, 1992.

[13] W. L. Bradley, C. R. Corleto, and D. P. Goetz, "Fracture physics of delamination of composite materials," *Composite Materials*, vol. 33, 1999.

[14] S. Mall, G. E. Law, and M. Katouzian, "Loading rate effect on interlaminar fracture toughness of a thermoplastic composite," *Journal of Composite Materials*, vol. 21, 1986/02/01.

[15] G. C. Jacob, J. M. Starbuck, J. F. Fellers, S. Simunovic, and R. G. Boeman, "The effect of loading rate on the fracture toughness of fiber reinforced polymer composites," *Journal of Applied Polymer Science*, vol. 96, 2005/05/05.

[16] A. Smiley and R. Pipes, "Rate effects on mode i interlaminar fracture toughness in composite materials," *Journal of Composite Materials*, vol. 21, pp. 670–687, 1987.

[17] S. Yarlagadda, A. AbuObaid, M. K. Yoon, N. Hager, and R. Domszy, "An automated technique for measuring crack propagation during mode i dcb testing," 2004.

[18] V. Ranatunga and S. B. Clay, "Cohesive modeling of damage growth in z-pinned laminates under mode-i loading," *Journal of Composite Materials*, vol. 47, pp. 3269–3283, 2012.

[19] I. K. Partridge, "Delamination behaviour of z-pinned laminates," *European Structural Integrity Society*, vol. 27, p. 2736, 2000.

[20] C. A. Steeves and N. A. Fleck, "In-plane properties of composite laminates with through-thickness pin reinforcement," *International Journal of Solids and Structures*, vol. 43, p. 31973212, 2006.

[21] A. Mouritz, K. Leong, and I. Herszberg, "A review of the effect of stitching on the in-plane mechanical properties of fibre-reinforced polymer composites," *Composites Part A: Applied Science and Manufacturing*, vol. 28, p. 979991, 1997.

[22] J. Blanco, E. J. Garcia, R. G. de Villoria, and B. L. Wardle, "Limiting mechanisms in mode i interlaminar toughness of composites reinforced with aligned carbon nanotubes," *Journal of Composite Materials*, vol. 43, pp. 825–841, 2009.

[23] F. Herrick, R. Casebier, J. Hamilton, and K. Sandberg, "Microfibrillated cellulose: Morphology and accessibility," *Applied Polymer Sci: Appl Polym Symposium*, vol. 37, p. 797813, 1983.

[24] A. Turbak, F. Snyder, and K. Sandberg, "Microfibrillated cellulose, a new cellulose product: properties, uses, and commercial potential, journal =,"

[25] A. M and L. T, "On the manufacture and uses of nanocellulose," *9th International Conference on Wood And Biofiber Plastic Composites*, 2007.

[26] H. Alamri and I. M. Low, "Characterization of epoxy hybrid composites filled with cellulose fibers and nano-sic," *Journal of Applied Polymer Science*, vol. 136, pp. E222–E232, 25 October 2012.

[27] K. Benhamou, hamid Kaddami, A. Magnin, A. Dufresne, and A. Ahmad, "Bio-based polyurethane reinforced with cellulose nanofibers: A comprehensive investigation on the effect of interface (pdf download available)," *Carbohydrate Polymers*, vol. in press, 2015/01/14.

[28] T. Saito, S. Kimura, Y. Nishiyama, and A. Isogai, "Cellulose nanofibers prepared by tempo-mediated oxidation of native cellulose," *Biomacromolecules*, vol. 8, 2007/09/01.

[29] Y. Wang, Z. Iqbal, and S. Mitra, "Rapidly functionalized, water-dispersed carbon nanotubes at high concentration," *American Chemical Society*, December 14, 2005.

[30] E. D. Aldo Arrais, D. Pezzini, R. Rossetti, and E. Boccaleri, "A fast effective route to ph-dependent water-dispersion of oxidized single-walled carbon nanotubes," *Carbon*, vol. 44, 2006/03/01.

[31] V. A. Sinani, M. K. Gheith, A. A. Yaroslavov, A. A. Rakhnyanskaya, K. Sun, A. A. Mamedov, J. P. Wicksted, and N. A. Kotov, "Aqueous dispersions of single-wall and multiwall carbon nanotubes with designed amphiphilic polycations (pdf download available)," *Journal of the American Chemical Society*, vol. 127, 2005/04/01.

[32] J. Lee, M. Kim, C. K. Hong, and S. E. Shim, "Measurement of the dispersion stability of pristine and surface-modified multiwalled carbon nanotubes in various nonpolar and polar solvents," *Measurement Science and Technology*.

Appendix A

This code is used to extract crack length data for a DCB specimen, output crack-length vs. time, compute fracture toughness, output fracture toughness, and plot crosshead load and crack length vs. crosshead displacement.

This code requires the MATLink package (http://matlink.org/) since it has embedded MATLAB code. The video file must be a .MOV file.

```
ClearAll["Global`*"]
Needs["MATLink`"]
Quiet[OpenMATLAB[]]
MEvaluate["clear all"]
Needs["MPlot`"]
safeExport[file_String, args___] :=
 If[! FileExistsQ[file] || ChoiceDialog["File already exists. Overwrite?"],
  Export[file, args], $Failed]

CreateDialog[{TextCell["Input video path:"],
   FileNameSetter[Dynamic[path], WindowTitle → "Select video file"],
   TextCell["Input data path:"], FileNameSetter[Dynamic[path2],
    WindowTitle → "Select data file"], DefaultButton[DialogReturn[
    ]]
  }];

len = Import[path, "FrameCount"];
Framed[Dynamic@N[100 (i / len)]]

{time, load, position} = (Import[path2][[2 ;;]] // Transpose)[[1 ;; 3]];
video = Table[Import[path, {"Frames", {i}}], {i, 1, len, 100}];
Beep[];

pts = {};
speclen = 5;
CreateDialog[{TextCell["click the left and right ends of the DCB sample: "],
   ClickPane[Dynamic@Show[Image[video[[1]], ImageSize → Large], Graphics[Table[
        {{Red, Green}[[i]], PointSize[0.01], Point[pts[[i]]]}, {i, Length[pts]}]]],
    If[Length[pts] < 2, AppendTo[pts, #]] &], TextCell["Input specimen length: "],
   InputField[Dynamic@speclen], DefaultButton[DialogReturn[left = pts[[1]][[1]];
     right = pts[[2]][[1]];
     pixlen = right - left;
     inperpix = speclen / pixlen]]
  }];

i = 1;
If[ValueQ[video], lineheight = (ImageDimensions@video[[1]])[[2]];
  inc = True;
  allow = False;
```

```
  tip = Table[{left + 2 / inperpix, 0}, {Length[video]}];
Framed@
 Column[{Row[{Button["Reset", tip = Table[{left + 2 / inperpix, 0}, {Length[video]}];
      i = 1, ImageSize → Small],
     Button["load", CreateDialog[{TextCell["Input crack data path:"],
        FileNameSetter[Dynamic[path3], WindowTitle → "Select crack data file"],
        TextCell["Input data path:"], FileNameSetter[Dynamic[path2],
         WindowTitle → "Select data file"], DefaultButton[DialogReturn[
          {ctime, clen} = Delete[#, 1] & /@ Transpose@(Import[path3][[1]]);
          {time, load, position} = (Import[path2][[2 ;;]] // Transpose)[[1 ;; 3]];
          MEvaluate["clear all"];
          MSet["crosshead_time", time];
          MSet["crosshead_load", load];
          MSet["crosshead_position", position];
          MSet["crack_time", ctime];
          MSet["crack_len", clen];
          MSet["plottitle", StringSplit[path2, "\\" | "."][[-2]]];
         ]]
       }], ImageSize → Small]}],
   Row[{Button["<<", Dynamic[If[i > 1, i = i - 1]]], InputField[Dynamic[i]],
     Button[">>", Dynamic[If[i < len, i = i + 1]]], Column[{"incremement on click",
       Checkbox[Dynamic[inc]], "allow crack<2\"", Checkbox[Dynamic[allow]]}]}],
   Pane@Row[{EventHandler[Dynamic@If[ValueQ[i] && ValueQ[video],
       Show[video[[i]], Graphics@
         {Red, Thin, Line[{{tip[[i]][[1]], 0}, {tip[[i]][[1]], lineheight}}]},
        ImageSize → Large], Graphics@Rectangle[{0, 0}, {1, 1}]],
      {"MouseDown" :> (If[(MousePosition["Graphics"][[1]] > left + 2 / inperpix) ||
           allow, tip[[i]] = MousePosition["Graphics"]];
         If[inc && i < Length[video], i = i + 1, framerate =
          Round[len / Import[path, "Duration"]];
         {ctime, clen} = Transpose@Table[{(100 / framerate) t,
             (tip[[t]][[1]] - left) inperpix}, {t, Length[video] - 1}];
          MSet["crosshead_time", time];
          MSet["crosshead_load", load];
          MSet["crosshead_position", position];
          MSet["crack_time", ctime];
          MSet["crack_len", clen];
          MSet["frame_rate", framerate];
          MSet["plottitle", StringSplit[path2, "\\" | "."][[-2]]])}],
    Dynamic@Magnify[If[ValueQ[i] && ValueQ[video],
       Show[ImageTake[video[[i]], -{MousePosition[{"Graphics", Pane}, {31, 31}][[
            2]], MousePosition[{"Graphics", Pane}, {31, 31}][[2]]} + {-30, 30},
         {MousePosition[{"Graphics", Pane}, {31, 31}][[1]],
```

```
        MousePosition[{"Graphics", Pane}, {31, 31}][[1]]} + {-30, 30}],
      Graphics@{Red, Thin, Line[{{31, 1}, {31, 62}}]}],
     Graphics@Rectangle[{0, 0}, {1, 1}]], 3]}],
 Dynamic@If[ValueQ[video], ListPlot[Table[{(100 / 24) t,
     (tip[[t]][[1]] - left) inperpix}, {t, Length[video] - 1}], ImageSize → Large,
   AxesOrigin → {0, 0}], Graphics@Rectangle[{0, 0}, {1, 1}]]}]
```

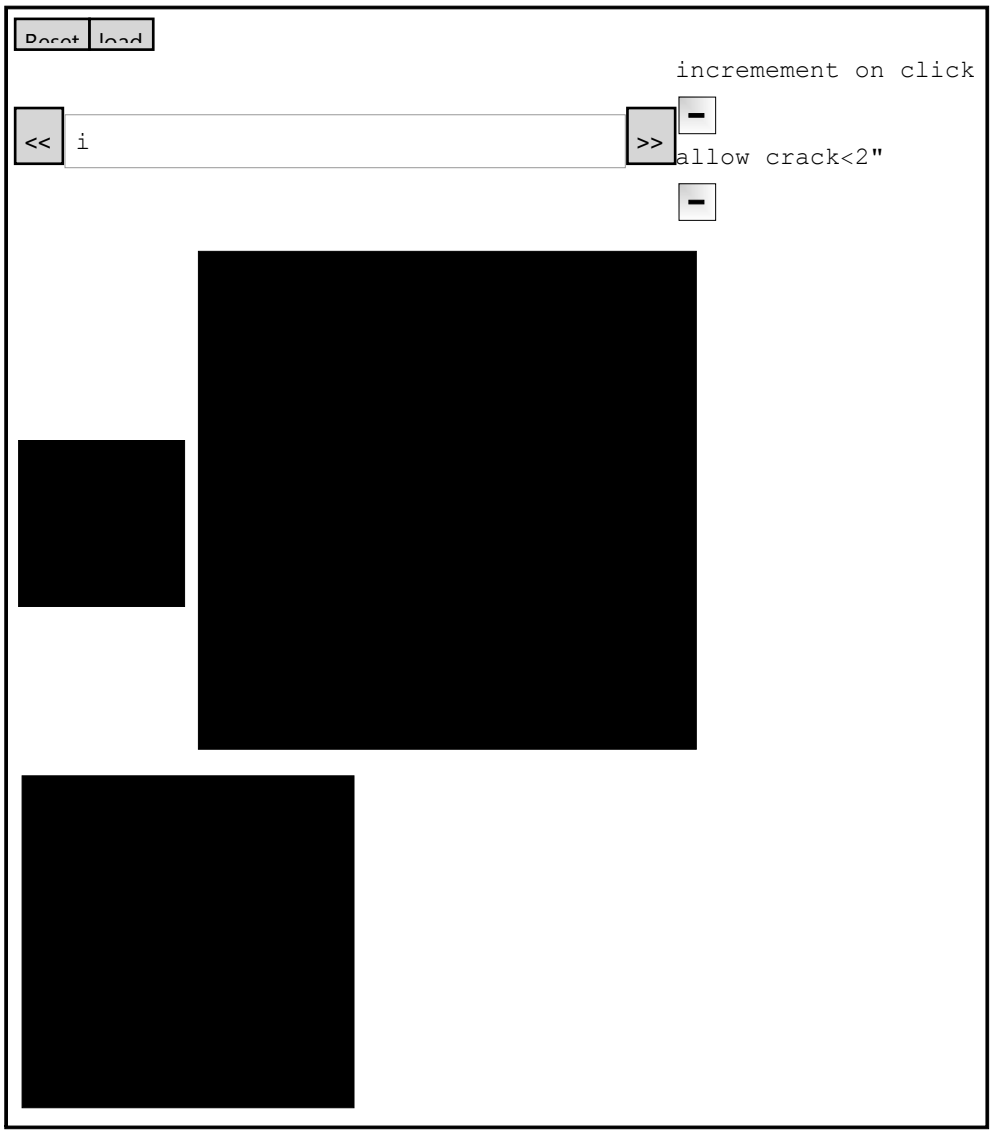


```
safeExport[NotebookDirectory[] <> "crack" <> StringSplit[path2, "\\" | "."][[-2]] <>
  ".xls", Transpose@{Prepend[ctime, "time"], Prepend[clen, "length"]}]
```

```
C:\Users\Seth\Documents\crackw3.xls
```

```
MPrint[1]
MPrint[2]
```

```
clc
hold on
```

```
figure(1)
grid on
hAx=plotyy((1/600)*(crack_time),2.54*crack_len,(1/600)*(crosshead_time),crosshead_lo
ad);%1/600*time converts to crosshead position
title(['Crack Length and Crosshead Loading, ' plottitle])
xlabel('Crosshead Position (cm)')
ylabel(hAx(1),'Crack Length (cm)') % left y-axis
ylabel(hAx(2),'Load (N)') % right y-axis
legend('crack growth','Load')
set(hAx(1),'YTick',linspace(0,ceil(1.1*2.54*max(crack_len)),9))
set(hAx(2),'YTick',linspace(0,ceil(1.1*max(crosshead_load)),11))
axis(hAx(1),[0 ceil(max((1/600)*(crack_time))) 0 ceil(1.1*2.54*max(crack_len))])
axis(hAx(2),[0 ceil(max((1/600)*(crack_time))) 0 ceil(1.1*max(crosshead_load))])
figure(2)
hold on
ratio=round(length (crosshead_time)/length(crack_time));

crosshead_loadvec=crosshead_load(1:ratio:length(crosshead_time));
crosshead_timevec=crosshead_time(1:ratio:length(crosshead_time));
crack_vec=crack_len(1:min([length(crosshead_timevec) length(crack_len)]));
crosshead_loadvec=crosshead_loadvec(1:min([length(crosshead_timevec)
length(crack_len)]));
crosshead_timevec=crosshead_timevec(1:min([length(crosshead_timevec)
length(crack_len)]));
moi = (1/12)*2.54*(2.54*0.15)^3;
EE= 61e6;

c = (2*(2.54*crack_vec.^3))./(3*EE*moi);

fit = polyfit(2.54*crack_vec,c.^(1/3),1);
m=fit(1);b=fit(2);

plot(2.54*crack_vec,c.^(1/3),'bo')
plot(linspace(0,2.54*crack_vec(end),5),m*linspace(0,2.54*crack_vec(end),5)+b,'g','Li
neWidth',2)
title(['R-curve ' plottitle])
xlabel('a (cm)')
ylabel('c^1^/^3')

figure(3)
hold on

G_i = (3*crosshead_loadvec.*(crosshead_timevec/600))./(2*2.54*(2.54*crack_vec));
%plot((2.54*crack_vec),G_i,'ro')
title(['Fracture Toughness ' plottitle])
xlabel('a (cm)')
ylabel('G_i')
grid on

current=crack_vec(1);
```

```
crack_top(1)=current;
G_i_top(1)=0;
max_G_i=0;
count=2;
for(i=1:length(crack_vec))

if((crack_vec(i)-current)>0.01)%||crack_vec(i)==max(crack_vec)
current = crack_vec(i);
crack_top(count)=crack_vec(i-1);
G_i_top(count)=max_G_i;
max_G_i=0;
count=count+1;

end

if(G_i(i)>max_G_i&&crack_vec(i)>0.1)
max_G_i=G_i(i);
end

end

crack_top(count)=crack_vec(end);
G_i_top(count) = G_i(end);

hold on
plot((2.54*crack_top),G_i_top,'b-')
title(['Fracture Toughness ' plottitle])
xlabel('a (cm)')
ylabel('G_i')
crack_top_export = (2.54*crack_top);
%axis([0 max(2.54*crack_top) 0 1.2*max(G_i_top)])
```

```
ListLinePlot[Transpose@{Prepend[MGet["crack_top_export"], "Crack Length"],
    Prepend[MGet["G_i_top"], "Fracture Toughness"]}]
```

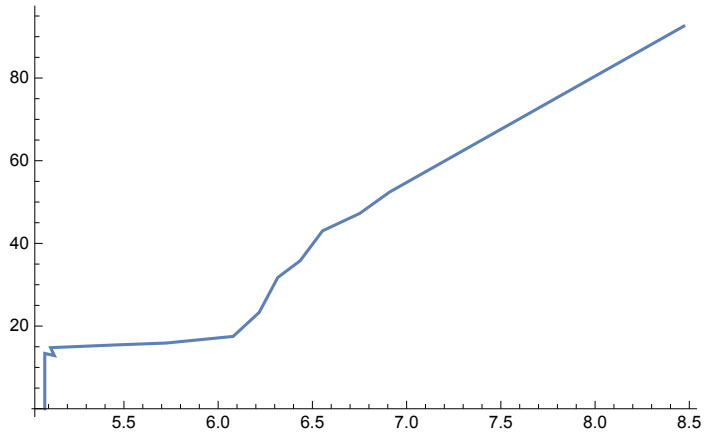

Appendix B

This code takes an excel file containing crosshead load vs. time for multiple samples, and plots the average crosshead loading with error regions. Samples that break early are dropped from consideration.

```
ClearAll["Global`*"]
```

Browse...

```
(*Determine the number of data sets and the number of columns per set*)
ycol = 2;
xcol = 3;
headers = Import[path, {"Data", 1, 1, All}];
xlabel = headers[[xcol]];
ylabel = headers[[ycol]];
temp = Flatten[Position[headers, headers[[1]]]];
sets = Length[temp];
temp = Table[temp[[i + 1]] - temp[[i]], {i, sets - 1}];
If[! Count[temp, temp[[1]]] == Length[temp], Print["Invalid Data"]]
types = temp[[1]];
yval = Table[{}, {sets}];

(*Import data by column*)
For[i = 1, i ≤ sets, i = i + 1,
 yval[[i]] = Import[path, {"Data", 1, All, ycol + types (i - 1)}];
 (*Eliminates headers*)
 yval[[i]] = Delete[yval[[i]], 1];
]
(*Eliminates empty data points*)
yval = DeleteCases[DeleteCases[yval, "", 3], {}, 2];

(*Eliminates data recorded after end of test*)
For[i = 1, i ≤ sets, i = i + 1,
 max = Max[yval[[i]]];
 maxpos = (Position[yval[[i]], max, 1, 1] // Flatten)[[1]];
 If[Count[yval[[i]][[maxpos ;;]], x_ /; x < 0.05 max, 1] == 0,
  endpos = Length[yval[[i]]] - maxpos, endpos =
   (Position[yval[[i]][[maxpos ;;]], x_ /; x < 0.05 max, 1, 1] // Flatten)[[1]]];
 yval[[i]] = yval[[i]][[1 ;; (maxpos + endpos)]];
]

num = Max[Length /@ yval];
ynd = Table[{}, {sets}];
For[j = 1, j ≤ sets, j = j + 1,
 ynd[[j]] = Append[yval[[j]], Table[0, {num - Length[yval[[j]]]}]] // Flatten;
]
```

```
stdev = Table[0, {num}];
mean = Table[0, {num}];
error = Table[0, {num}];
For[j = 1, j ≤ num, j = j + 1,
 set = DeleteCases[Table[ynd[[i]][[j]], {i, 1, sets}], 0];
 mean[[j]] = Mean[set];
 len = Length@set;
 If[len > 1,
  stdev[[j]] = StandardDeviation[set];
 ];
 error[[j]] = stdev[[j]] / len;
]

xval = Import[path, {"Data", 1, All, xcol}];
(*Eliminates headers*)
xval = Delete[xval, 1];
xval = DeleteCases[DeleteCases[xval, ""], {}];
dx = Mean[xval[[2 ;; -1]] - xval[[1 ;; -2]]];

Beep[]
```

```
Rasterize@Framed@Column[{
     Style["Wet-flocked CNT Samples", Larger],
     Row[{
       ListLinePlot[{
         Transpose[{Table[i dx, {i, num}], mean}],
         Transpose[{Table[i dx, {i, num}], mean + stdev}],
         Transpose[{Table[i dx, {i, num}], mean - stdev}],
         Transpose[{Table[i dx, {i, num}], mean + error}],
         Transpose[{Table[i dx, {i, num}], mean - error}]}, PlotStyle →
         {{Darker@Blue, Thin}, Transparent, Transparent, Transparent, Transparent},
        Filling → {1 → {{2}, LightBlue}, 1 → {{3}, LightBlue}, 1 → {{4}, Lighter@Blue},
          1 → {{5}, Lighter@Blue}}, AxesLabel → {xlabel, ylabel},
        PlotLabel → Style["Average DCB test", {Large, Bold}], ImageSize → Medium],
       Framed[{{"mean", Darker@Blue}, {"± standard error", Lighter@Blue},
          {"± standard deviation", LightBlue}} // TableForm]
      }],
     Row[{
       Show@Table[ListPlot[Transpose[{Table[i dx, {i, num}], ynd[[l]]}],
          Joined → True, PlotStyle → {Thin, RGBColor[l / sets, 1 - l / sets, 0]},
          ImageSize → Medium, AxesLabel → {xlabel, ylabel},
          PlotLabel → Style["Individual DCB test", {Large, Bold}],
          PlotRange → {{0, num dx}, {0, Max@(Max /@ ynd)}}], {l, sets}],
       Framed[Table[{"sample" <> ToString@l, RGBColor[l / sets, 1 - l / sets, 0]},
          {l, 1, sets}] // TableForm]
      }](*,
     Row[{
       ListLinePlot[{stdev,error},PlotStyle→{Transparent,Transparent},
        PlotLabel→Style["DCB test Error",{Large,Bold}],ImageSize→Medium,
        Filling→{1→{Axis,Lighter@Blue},1→{{2},LightBlue}}],
       Framed[{{" standard error",Lighter@Blue},
          {"standard deviation",LightBlue}}//TableForm]
      }]*)
    }]
```

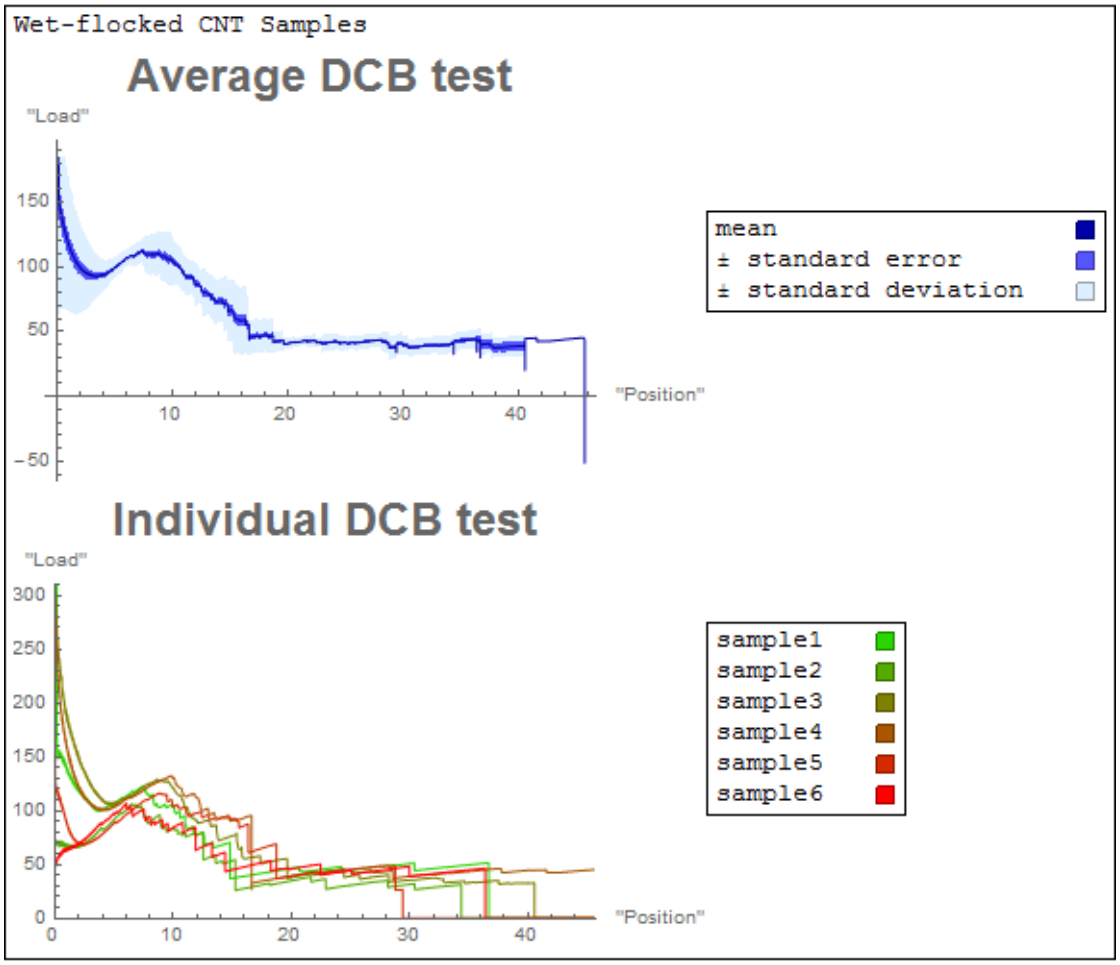
Wet-flocked CNT Samples
Average DCB test
"Load"
150
100
50
−50
10
20
30
40
"Position"
mean
± standard error
± standard deviation
Individual DCB test
"Load"
300
250
200
150
100
50
0
0
10
20
30
40
"Position"
sample1
sample2
sample3
sample4
sample5
sample6

```
Framed@Column[{
    Style["Sewn Z-pinned Samples", Larger],
    Row[{
      ListLinePlot[{
        Transpose[{Table[i dx, {i, num}], mean}]}, PlotStyle → {{Darker@Blue, Thin}},
       AxesLabel → {xlabel, ylabel}, ImageSize → Medium]
     }]
  }]
```

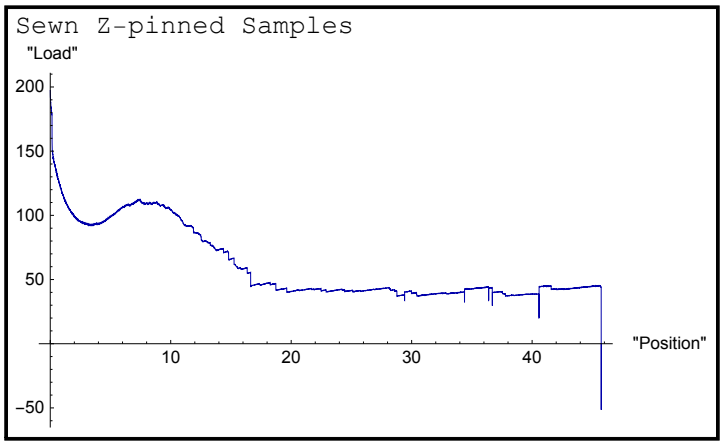

Appendix C

This code takes an excel file containing fracture toughness data for multiple specimens, and plots the average fracture toughness. Linear interpolation between datapoints is used.

```
ClearAll["Global`*"]
```

Browse...

```
(*Determine the number of data sets and the number of columns per set*)
ycol = 2;
xcol = 1;
headers = Import[path, {"Data", 1, 1, All}];
xlabel = headers[[xcol]];
ylabel = headers[[ycol]];
temp = Flatten[Position[headers, headers[[1]]]];
sets = Length[temp];
temp = Table[temp[[i + 1]] - temp[[i]], {i, sets - 1}];
If[! Count[temp, temp[[1]]] == Length[temp], Print["Invalid Data"]]
types = temp[[1]];
yval = Table[{}, {sets}];
xval = Table[{}, {sets}];
(*Import data by column*)
For[i = 1, i ≤ sets, i = i + 1,
 yval[[i]] = Import[path, {"Data", 1, All, ycol + types (i - 1)}];
 (*Eliminates headers*)
 yval[[i]] = Delete[yval[[i]], 1];
 xval[[i]] = Import[path, {"Data", 1, All, xcol + types (i - 1)}];
 (*Eliminates headers*)
 xval[[i]] = Delete[xval[[i]], 1];
]
xval = DeleteCases[xval, _String, 2];
yval = DeleteCases[yval, _String, 2];
xmax = Max@Flatten@xval;
y[x_] =
  Table[Piecewise[Table[{Normal[LinearModelFit[{{xval[[j]][[i]], yval[[j]][[i]]},
         {xval[[j]][[i + 1]], yval[[j]][[i + 1]]}}, x, x]], x > xval[[j]][[i]] &&
       x < xval[[j]][[i + 1]]}, {i, 1, Length[xval[[j]]] - 1}]], {j, 1, sets}];
title = Capitalize@StringSplit[StringSplit[path, RegularExpression[".*frac"]][[
     1]], RegularExpression["[.]xlsx"]][[1]]
```

```
Water
```

```
ListLinePlot[Table[Transpose@{xval[[i]], yval[[i]]}, {i, sets}],
 PlotLabel → "Fracture Toughness, Water-Control",
 AxesLabel → {"Crack length (cm)", "Gi"}]
Plot[Mean@DeleteCases[y[x], _?(# < 1 &)], {x, 0, xmax}, Exclusions → {True},
 PlotLabel → "Average Fracture Toughness, Water-Control",
 AxesLabel → {"Crack length (cm)", "Gi"},
 AxesOrigin → {0, 0}, PlotStyle → Darker@Blue]
```